critical for the transcriptional activity of Tat (18). Another study demonstrated that ORF45 of the Kaposi's sarcoma-associated herpesvirus interacts with RSK1 and RSK2, resulting in their stimulation (22). Further studies suggest that RSK1/2 upregulation plays a critical role in the lytic replication of Kaposi's sarcoma-associated herpesvirus (22). Another study suggested that RSK2 signaling is important for efficient vaccinia virus amplification (1). It is interesting to note that these studies ascribe a virus-supportive role to RSK2 activation.

In contrast to the above-mentioned studies, which found a virus-supportive role for RSK2, our findings suggest an antiviral activity for this kinase. In particular, we found that the C-terminal domain of RSK2, which acts in a dominant-negative manner, and a small interfering RNA to RSK2 increased influenza virus polymerase activity in in vitro assays and/or enhanced influenza virus replication. RSK2 is known to be activated by the Raf/MEK/ERK signaling cascade (reviewed in reference 24). Studies by Pleschka et al. (39) suggest that this pathway has a virus-supportive function. This finding seems to contradict our finding that RSK2 has antiviral activity. However, the virus-supportive function of the Raf/MEK/ERK signaling cascade was established by use of an inhibitor to MEK (39), which may affect several pathways that are controlled by MEK/ERK. In addition, activation of RSK1/2 is controlled not only by ERK1/2, but also by other MAPKs, such as p38 (reviewed in references 10 and 40), which is activated upon influenza virus infection and triggers an antiviral response (8). Collectively, the current data suggest that RSK2 is activated by both virus-supportive and -antagonistic signaling pathways and that the complex interplay of these factors and pathways determines its downstream effects.

Our data suggest that RSK2 may execute its antiviral function through NF-κB. Some studies have found a supportive role for NF-κB in influenza virus infection (32, 50), while another study suggested that NF-κB activation is not required for efficient influenza virus replication (5). In general, the role of NF-κB in the regulation of IFN-β responses is still not well understood. Recent studies found that NF-κB stimulates the expression of certain IFN-stimulated genes, while it suppresses others (37). As discussed earlier, viral infections trigger multiple cellular pathways that stimulate both agonistic and antagonistic functions; the outcome of a viral infection may ultimately be determined by the complex and as yet poorly understood interplay between these virus-supportive and -antagonistic factors.

We found that RSK2 affects influenza virus replication through innate immune response pathways (Fig. 6). Although RSK2 is known to activate NF-κB (13, 43) and PKR (53), it had not been recognized as a critical signaling component in innate immune responses to viral infections. We found, however, that RSK2 knockdown in 293 cells affected the influenza virus-induced activation of NF-κB and IFN-β and the influenza virus-induced phosphorylation of PKR, suggesting a critical role for RSK2 in innate immune responses to viral infections. In fact, we found that RSK2 knockdown not only increased influenza A virus titers but also stimulated influenza B virus and Sendai virus replication. In conclusion, we have identified a role for RSK2 in innate immune responses to influenza A virus infection, which may be executed through the regulation of IFN-β, NF-κB, and PKR responses. Other MAPK-activated protein kinases may have similar, as of yet unidentified, functions in the innate immune response and antiviral defense mechanisms.

ACKNOWLEDGMENTS

We thank Susan Watson for editing the manuscript and Hideo Iba for providing us with plasmids for the retroviral vector-mediated RNA interference studies.

This research was supported by grants-in-aid from the Ministry of Education, Culture, Sports, Science, and Technology of Japan, by ERATO (Japan Science and Technology Agency), and by National Institute of Allergy and Infectious Diseases Public Health Service research grants.

REFERENCES

1. **Andrade, A. A., P. N. Silva, A. C. Pereira, L. P. De Sousa, P. C. Ferreira, R. T. Gazzinelli, E. G. Kroon, C. Ropert, and C. A. Bonjardim.** 2004. The vaccinia virus-stimulated mitogen-activated protein kinase (MAPK) pathway is required for virus multiplication. Biochem. J. **381**:437–446.
2. **Balachandran, S., P. C. Roberts, L. E. Brown, H. Truong, A. K. Pattnaik, D. R. Archer, and G. N. Barber.** 2000. Essential role for the dsRNA-dependent protein kinase PKR in innate immunity to viral infection. Immunity **13**:129–141.
3. **Barber, G. N.** 2005. The dsRNA-dependent protein kinase, PKR and cell death. Cell Death Differ. **12**:563–570.
4. **Bergmann, M., A. Garcia-Sastre, E. Carnero, H. Pehamberger, K. Wolff, P. Palese, and T. Muster.** 2000. Influenza virus NS1 protein counteracts PKR-mediated inhibition of replication. J. Virol. **74**:6203–6206.
5. **Bernasconi, D., C. Amici, S. La Frazia, A. Ianaro, and M. G. Santoro.** 2005. The IkappaB kinase is a key factor in triggering influenza A virus-induced inflammatory cytokine production in airway epithelial cells. J. Biol. Chem. **280**:24127–24134.
6. **Carriere, A., H. Ray, J. Blenis, and P. P. Roux.** 2008. The RSK factors of activating the Ras/MAPK signaling cascade. Front. Biosci. **13**:4258–4275.
7. **Chen, R. H., C. Sarnecki, and J. Blenis.** 1992. Nuclear localization and regulation of *erk*- and *rsk*-encoded protein kinases. Mol. Cell. Biol. **12**:915–927.
8. **Conze, D., J. Lumsden, H. Enslen, R. J. Davis, G. Le Gros, and M. Rincón.** 2000. Activation of p38 MAP kinase in T cells facilitates the immune response to the influenza virus. Mol. Immunol. **37**:503–513.
9. **Donelan, N. R., C. F. Basler, and A. García-Sastre.** 2003. A recombinant influenza A virus expressing an RNA-binding-defective NS1 protein induces high levels of beta interferon and is attenuated in mice. J. Virol. **77**:13257–13266.
10. **Gaestel, M.** 2008. Specificity of signaling from MAPKs to MAPKAPKs: kinases' tango nuevo. Front. Biosci. **13**:6050–6059.
11. **Gale, M., Jr., and M. G. Katze.** 1998. Molecular mechanisms of interferon resistance mediated by viral-directed inhibition of PKR, the interferon-induced protein kinase. Pharmacol. Ther. **78**:29–46.
12. **Geiss, G. K., M. Salvatore, T. M. Tumpey, V. S. Carter, X. Wang, C. F. Basler, J. K. Taubenberger, R. E. Bumgarner, P. Palese, M. G. Katze, and A. García-Sastre.** 2002. Cellular transcriptional profiling in influenza A virus-infected lung epithelial cells: the role of the nonstructural NS1 protein in the evasion of the host innate defense and its potential contribution to pandemic influenza. Proc. Natl. Acad. Sci. USA **99**:10736–10741.
13. **Ghoda, L., X. Lin, and W. C. Greene.** 1997. The 90-kDa ribosomal S6 kinase (pp90rsk) phosphorylates the N-terminal regulatory domain of IkappaBalpha and stimulates its degradation in vitro. J. Biol. Chem. **272**:21281–21288.
14. **Goodman, A. G., J. A. Smith, S. Balachandran, O. Perwitasari, S. C. Proll, M. J. Thomas, M. J. Korth, G. N. Barber, L. A. Schiff, and M. G. Katze.** 2007. The cellular protein P58IPK regulates influenza virus mRNA translation and replication through a PKR-mediated mechanism. J. Virol. **81**:2221–2223.
15. **Haller, O., G. Kochs, and F. Weber.** 2007. Interferon, Mx, and viral countermeasures. Cytokine Growth Factor Rev. **18**:425–433.
16. **Hatta, M., P. Gao, P. Halfmann, and Y. Kawaoka.** 2001. Molecular basis for high virulence of Hong Kong H5N1 influenza A viruses. Science **293**:1840–1842.
17. **Hatta, M., Y. Hatta, J. H. Kim, S. Watanabe, K. Shinya, T. Nguyen, P. S. Lien, Q. M. Le, and Y. Kawaoka.** 2007. Growth of H5N1 influenza A viruses in the upper respiratory tracts of mice. PLoS Pathog. **3**:1374–1379.
18. **Hetzer, C., D. Bisgrove, M. S. Cohen, A. Pedal, K. Kaehlcke, A. Speyerer, K. Bartscherer, J. Taunton, and M. Ott.** 2007. Recruitment and activation of RSK2 by HIV-1 Tat. PLoS ONE **2**:e151.
19. **Hiscott, J., H. Kwon, and P. Génin.** 2001. Hostile takeovers: viral appropriation of the NF-kappaB pathway. J. Clin. Investig. **107**:143–151.
20. **Kitamura, T., and Y. Morikawa.** 2000. Isolation of T-cell antigens by retrovirus-mediated expression cloning. Methods Mol. Biol. **134**:143–152.
21. **Kochs, G., A. García-Sastre, and L. Martínez-Sobrido.** 2007. Multiple anti-

interferon actions of the influenza A virus NS1 protein. J. Virol. **81**:7011–7021.
22. **Kuang, E., Q. Tang, G. G. Maul, and F. Zhu.** 2008. Activation of p90 ribosomal S6 kinase by ORF45 of Kaposi's sarcoma-associated herpesvirus and its role in viral lytic replication J. Virol. **82**:1838–1850.
23. **Kujime, K., S. Hashimoto, Y. Gon, K. Shimizu, and T. Horie.** 2000. p38 mitogen-activated protein kinase and c-jun-NH2-terminal kinase regulate RANTES production by influenza virus-infected human bronchial epithelial cells. J. Immunol. **164**:3222–3228.
24. **Lu, Z., and S. Xu.** 2006. ERK1/2 MAP kinases in cell survival and apoptosis. IUBMB Life **58**:621–631.
25. **Ludwig, S., C. Ehrhardt, E. R. Neumeier, M. Kracht, U. R. Rapp, and S. Pleschka.** 2001. Influenza virus-induced AP-1-dependent gene expression requires activation of the JNK signaling pathway. J. Biol. Chem. **276**:10990–10998.
26. **Ludwig, S., O. Planz, S. Pleschka, and T. Wolff.** 2003. Influenza-virus-induced signaling cascades: targets for antiviral therapy? Trends Mol. Med. **9**:46–52.
27. **Ludwig, S., S. Pleschka, O. Planz, and T. Wolff.** 2006. Ringing the alarm bells: signalling and apoptosis in influenza virus infected cells. Cell. Microbiol. **8**:375–386.
28. **Massin, P., S. van der Werf, and N. Naffakh.** 2001. Residue 627 of PB2 is a determinant of cold sensitivity in RNA replication of avian influenza viruses. J. Virol. **75**:5398–5404.
29. **Mibayashi, M., L. Martínez-Sobrido, Y. M. Loo, W. B. Cárdenas, M. Gale, Jr., and A. García-Sastre.** 2007. Inhibition of retinoic acid-inducible gene I-mediated induction of beta interferon by the NS1 protein of influenza A virus. J. Virol. **81**:514–524.
30. **Min, J. Y., and R. M. Krug.** 2006. The primary function of RNA binding by the influenza A virus NS1 protein in infected cells: inhibiting the 2′-5′ oligo(A) synthetase/RNase L pathway. Proc. Natl. Acad. Sci. USA **103**:7100–7105.
31. **Neumann, G., T. Watanabe, H. Ito, S. Watanabe, H. Goto, P. Gao, M. Hughes, D. R. Perez, R. Donis, E. Hoffmann, G. Hobom, and Y. Kawaoka.** 1999. Generation of influenza A viruses entirely from cloned cDNAs. Proc. Natl. Acad. Sci. USA **96**:9345–9350.
32. **Nimmerjahn, F., D. Dudziak, U. Dirmeier, G. Hobom, A. Riedel, M. Schlee, L. M. Staudt, A. Rosenwald, U. Behrends, G. W. Bornkamm, and J. Mautner.** 2004. Active NF-kappaB signalling is a prerequisite for influenza virus infection. J. Gen. Virol. **85**:2347–2356.
33. **Niwa, H., K. Yamamura, and J. Miyazaki.** 1991. Efficient selection for high-expression transfectants with a novel eukaryotic vector. Gene **108**:193–199.
34. **Onishi, M., S. Kinoshita, Y. Morikawa, A. Shibuya, J. Phillips, L. L. Lanier, D. M. Gorman, G. P. Nolan, A. Miyajima, and T. Kitamura.** 1996. Applications of retrovirus-mediated expression cloning. Exp. Hematol. **24**:324–329.
35. **Pahl, H. L., and P. A. Baeuerle.** 1995. Expression of influenza virus hemagglutinin activates transcription factor NF-κB. J. Virol. **69**:1480–1484.
36. **Palese, P.** 2007. Orthomyxoviridae, p. 1649–1689. *In* D. M. Knipe, P. M. Howley, D. E. Griffin, R. A. Lamb, M. A. Martin, B. Roizman, and S. E. Straus (ed.), Fields virology, 5th ed. Lippincott Williams & Wilkins, Philadelphia, PA.
37. **Pfeffer, L. M., J. G. Kim, S. R. Pfeffer, D. J. Carrigan, D. P. Baker, L. Wei, and R. Homayouni.** 2004. Role of nuclear factor-kappaB in the antiviral action of interferon and interferon-regulated gene expression. J. Biol. Chem. **279**:31304–31311.
38. **Pleschka, S.** 2008. RNA viruses and the mitogenic Raf/MEK/ERK signal transduction cascade. Biol. Chem. [Epub ahead of print] doi:10.1515/BC.2008.145.
39. **Pleschka, S., T. Wolff, C. Ehrhardt, G. Hobom, O. Planz, U. R. Rapp, and S. Ludwig.** 2001. Influenza virus propagation is impaired by inhibition of the Raf/MEK/ERK signalling cascade. Nat. Cell Biol. **3**:301–305.
40. **Raman, M., W. Chen, and M. H. Cobb.** 2007. Differential regulation and properties of MAPKs. Oncogene **26**:3100–3112.
41. **Roux, P. P., and J. Blenis.** 2004. ERK and p38 MAPK-activated protein kinases: a family of protein kinases with diverse biological functions. Microbiol. Mol. Biol. Rev. **68**:320–344.
42. **Roux, P. P., S. A. Richards, and J. Blenis.** 2003. Phosphorylation of p90 ribosomal S6 kinase (RSK) regulates extracellular signal-regulated kinase docking and RSK activity. Mol. Cell. Biol. **23**:4796–4804.
43. **Schouten, G. J., A. C. Vertegaal, S. T. Whiteside, A. Israël, M. Toebes, J. C. Dorsman, A. J. van der Eb, and A. Zantema.** 1997. IkappaB alpha is a target for the mitogen-activated 90 kDa ribosomal S6 kinase. EMBO J. **16**:3133–3144.
44. **Shimojima, M., T. Miyazawa, Y. Ikeda, E. L. McMonagle, H. Haining, H. Akashi, Y. Takeuchi, M. J. Hosie, and B. J. Willett.** 2004. Use of CD134 as a primary receptor by the feline immunodeficiency virus. Science **303**:1192–1195.
45. **Shimojima, M., T. Miyazawa, Y. Sakurai, Y. Nishimura, Y. Tohya, Y. Matsuura, and H. Akashi.** 2003. Usage of myeloma and panning in retrovirus-mediated expression cloning. Anal. Biochem. **315**:138–140.
46. **Shinya, K., S. Hamm, M. Hatta, H. Ito, T. Ito, and Y. Kawaoka.** 2004. PB2 amino acid at position 627 affects replicative efficiency, but not cell tropism, of Hong Kong H5N1 influenza A viruses in mice. Virology **320**:258–266.
47. **Subbarao, E. K., W. London, and B. R. Murphy.** 1993. A single amino acid in the PB2 gene of influenza A virus is a determinant of host range. J. Virol. **67**:1761–1764.
48. **Talon, J., C. M. Horvath, R. Polley, C. F. Basler, T. Muster, P. Palese, and A. García-Sastre.** 2000. Activation of interferon regulatory factor 3 is inhibited by the influenza A virus NS1 protein. J. Virol. **74**:7989–7996.
49. **Wang, X., M. Li, H. Zheng, T. Muster, P. Palese, A. A. Beg, and A. García-Sastre.** 2000. Influenza A virus NS1 protein prevents activation of NF-κB and induction of alpha/beta interferon. J. Virol. **74**:11566–11573.
50. **Wei, L., M. R. Sandbulte, P. G. Thomas, R. J. Webby, R. Homayouni, and L. M. Pfeffer.** 2006. NFkappaB negatively regulates interferon-induced gene expression and anti-influenza activity. J. Biol. Chem. **281**:11678–11684.
51. **Wright, P. F.** 2007. Orthomyxoviruses, p. 1691–1740. *In* D. M. Knipe, P. M. Howley, D. E. Griffin, R. A. Lamb, M. A. Martin, B. Roizman, and S. E. Straus (ed.), Fields virology, 5th ed. Lippincott Williams & Wilkins, Philadelphia, PA.
52. **Wurzer, W. J., C. Ehrhardt, S. Pleschka, F. Berberich-Siebelt, T. Wolff, H. Walczak, O. Planz, and S. Ludwig.** 2004. NF-kappaB-dependent induction of tumor necrosis factor-related apoptosis-inducing ligand (TRAIL) and Fas/FasL is crucial for efficient influenza virus propagation. J. Biol. Chem. **279**:30931–30937.
53. **Zykova, T. A., F. Zhu, Y. Zhang, A. M. Bode, and Z. Dong.** 2007. Involvement of ERKs, RSK2 and PKR in UVA-induced signal transduction toward phosphorylation of eIF2alpha (Ser(51)). Carcinogenesis **28**:1543–1551.

LETTERS

In vitro and *in vivo* characterization of new swine-origin H1N1 influenza viruses

Yasushi Itoh[1], Kyoko Shinya[2], Maki Kiso[3], Tokiko Watanabe[4], Yoshihiro Sakoda[5], Masato Hatta[4], Yukiko Muramoto[6], Daisuke Tamura[3], Yuko Sakai-Tagawa[3], Takeshi Noda[7], Saori Sakabe[3], Masaki Imai[4], Yasuko Hatta[4], Shinji Watanabe[4], Chengjun Li[4], Shinya Yamada[3], Ken Fujii[6], Shin Murakami[3], Hirotaka Imai[3], Satoshi Kakugawa[3], Mutsumi Ito[3], Ryo Takano[3], Kiyoko Iwatsuki-Horimoto[3], Masayuki Shimojima[3], Taisuke Horimoto[3], Hideo Goto[3], Kei Takahashi[3], Akiko Makino[2], Hirohito Ishigaki[1], Misako Nakayama[1], Masatoshi Okamatsu[5], Kazuo Takahashi[8], David Warshauer[9], Peter A. Shult[9], Reiko Saito[10], Hiroshi Suzuki[10], Yousuke Furuta[11], Makoto Yamashita[12], Keiko Mitamura[13], Kunio Nakano[13], Morio Nakamura[13], Rebecca Brockman-Schneider[14], Hiroshi Mitamura[15], Masahiko Yamazaki[16], Norio Sugaya[17], M. Suresh[4], Makoto Ozawa[4,7], Gabriele Neumann[4], James Gern[14], Hiroshi Kida[5], Kazumasa Ogasawara[1] & Yoshihiro Kawaoka[2,3,4,6,7,18]

Influenza A viruses cause recurrent outbreaks at local or global scale with potentially severe consequences for human health and the global economy. Recently, a new strain of influenza A virus was detected that causes disease in and transmits among humans, probably owing to little or no pre-existing immunity to the new strain. On 11 June 2009 the World Health Organization declared that the infections caused by the new strain had reached pandemic proportion. Characterized as an influenza A virus of the H1N1 subtype, the genomic segments of the new strain were most closely related to swine viruses[1]. Most human infections with swine-origin H1N1 influenza viruses (S-OIVs) seem to be mild; however, a substantial number of hospitalized individuals do not have underlying health issues, attesting to the pathogenic potential of S-OIVs. To achieve a better assessment of the risk posed by the new virus, we characterized one of the first US S-OIV isolates, A/California/04/09 (H1N1; hereafter referred to as CA04), as well as several other S-OIV isolates, *in vitro* and *in vivo*. In mice and ferrets, CA04 and other S-OIV isolates tested replicate more efficiently than a currently circulating human H1N1 virus. In addition, CA04 replicates efficiently in non-human primates, causes more severe pathological lesions in the lungs of infected mice, ferrets and non-human primates than a currently circulating human H1N1 virus, and transmits among ferrets. In specific-pathogen-free miniature pigs, CA04 replicates without clinical symptoms. The assessment of human sera from different age groups suggests that infection with human H1N1 viruses antigenically closely related to viruses circulating in 1918 confers neutralizing antibody activity to CA04. Finally, we show that CA04 is sensitive to approved and experimental antiviral drugs, suggesting that these compounds could function as a first line of defence against the recently declared S-OIV pandemic.

Sequence analyses of recently emerged swine-origin H1N1 viruses (S-OIVs) revealed the absence of markers associated with high pathogenicity in avian and/or mammalian species, such as a multibasic haemagglutinin (HA) cleavage site[2] or lysine at position 627 of the PB2 protein[3]. To characterize the new viruses *in vitro* and *in vivo*, we amplified the following S-OIVs in Madin–Darby canine kidney (MDCK) cells: A/California/04/09 (CA04), A/Wisconsin/WSLH049/09 (WSLH049), A/Wisconsin/WSLH34939/09 (WSLH34939), A/Netherlands/603/09 (Net603) and A/Osaka/164/09 (Osaka164). WSLH34939 was isolated from a patient who required hospitalization, whereas the remaining viruses were isolated from mild cases. These viruses represent the currently recognized neuraminidase (NA) variants among S-OIVs: CA04, NA-106V, NA-248N; Osaka164, NA-106I, NA-248N; WSLH049, NA-106I, NA-248D; WSLH34939, NA-106I, NA-248D; and Net603, NA-106V, NA-248N.

In MDCK cells and primary human airway epithelial cells, CA04 grew to titres comparable to those typically obtained for contemporary human H1N1 influenza viruses (Supplementary Fig. 1). Confocal, transmission electron and scanning electron microscopy revealed virions of remarkably filamentous shape (Supplementary Fig. 2), in marked contrast to the spherical shape observed with negatively stained virions (http://www.cdc.gov/h1n1flu/images.htm). The biological significance of the morphology of CA04 remains unknown.

To evaluate the pathogenicity of S-OIV in mammalian models, we conducted studies in mice, ferrets, non-human primates and pigs. BALB/c mice intranasally infected with a high dose ($>10^4$ plaque-forming units (p.f.u.)) of CA04 (Supplementary Fig. 3) experienced weight loss and those infected with the highest dose of this virus were humanely killed, in contrast to animals infected with a recent human H1N1 virus (A/Kawasaki/UTK-4/09, KUTK-4). The 50% mouse lethal dose (MLD_{50}) was $10^{5.8}$ p.f.u. for CA04 and $>10^{6.6}$ p.f.u. for

[1]Department of Pathology, Shiga University of Medical Science, Ohtsu, Shiga 520-2192, Japan. [2]Department of Microbiology and Infectious Diseases, Kobe University, Hyogo 650-0017, Japan. [3]Division of Virology, Department of Microbiology and Immunology, Institute of Medical Science, University of Tokyo, Tokyo 108-8639, Japan. [4]Department of Pathobiological Sciences, University of Wisconsin-Madison, Madison, Wisconsin 53711, USA. [5]Department of Disease Control, Graduate School of Veterinary Medicine, Hokkaido University, Sapporo 060-0818, Japan. [6]ERATO Infection-Induced Host Responses Project, Saitama 332-0012, Japan. [7]Department of Special Pathogens, International Research Center for Infectious Diseases, Institute of Medical Science, University of Tokyo, Tokyo 108-8639, Japan. [8]Department of Infectious Diseases, Osaka Prefectural Institute of Public Health, Osaka 537-0025, Japan. [9]Wisconsin State Laboratory of Hygiene, Madison, Wisconsin 53706, USA. [10]Department of Public Health, Niigata University, Graduate School of Medical and Dental Sciences, Niigata 951-8510, Japan. [11]Toyama Chemical Co., Ltd., Toyama 930-8508, Japan. [12]Daiichi Sankyo Co Ltd, Shinagawa, Tokyo 140-8710, Japan. [13]Eiju General Hospital, Tokyo 110-8654, Japan. [14]School of Medicine and Public Health, University of Wisconsin-Madison, Madison, Wisconsin 53792, USA. [15]Department of Internal Medicine, Mitamura Clinic, Shizuoka 413-0103, Japan. [16]Department of Pediatrics, Zama Children's Clinic, Kanagawa 228-0023, Japan. [17]Keiyu Hospital, Kanagawa 220-0012, Japan. [18]Creative Research Initiative, Sousei, Hokkaido University, Sapporo 060-0818, Japan.

KUTK-4. For the additional S-OIV isolates tested, the MLD_{50} values were $>10^{6.4}$ p.f.u. for Osaka164, $>10^{6.6}$ p.f.u. for WSLH049, $10^{4.5}$ p.f.u. for WSLH34939 and $>10^{5.8}$ p.f.u. for Net603.

On day 3 after infection of mice, similar titres were detected in nasal turbinates of mice infected with 10^5 p.f.u. of S-OIVs or KUTK-4 (Supplementary Table 1); however, S-OIVs replicated more efficiently in the lungs of infected animals, which may account for the prominent bronchitis and alveolitis with viral antigen on day 3 after infection with CA04 (Supplementary Fig. 4a, b). On day 6 after infection, virus titres followed a similar trend and the lungs of CA04-infected mice showed bronchitis and alveolitis with viral antigen, although signs of regeneration were apparent (Supplementary Fig. 4c). We detected viral-antigen-positive bronchial epithelial cells, but not alveolar cells, on day 3 after infection of mice infected with KUTK-4 (Supplementary Fig. 4e). By day 6, infection in KUTK-4-inoculated mice had progressed to bronchitis and peribronchitis; however, viral antigen was rarely detected in these lesions (Supplementary Fig. 4f).

There were marked differences in the induction of pro-inflammatory cytokines in the lungs of mice infected with CA04 compared with KUTK-4 (Supplementary Fig. 5a–c). Infection with KUTK-4 resulted in limited induction of pro-inflammatory cytokines/chemokines in the lungs, in marked contrast to infection with CA04. Increased production of interleukin-10 (IL-10; Supplementary Fig. 5a) in lungs of CA04-infected mice at day 6 after infection probably reflects a host response to dampen over-exuberant pulmonary inflammation and promote tissue repair. Infection with CA04 led to strong induction of both interferon-γ (IFN-γ) and IL-4 in the lungs. The selective induction of the T_H2 cytokine IL-5 in CA04-infected, but not in KUTK-4-infected, mice on day 6 after infection is noteworthy (Supplementary Fig. 5b), but further studies are needed to understand the relevance of this finding to viral control. IL-17 has been reported to have a role in protection against lethal influenza and also in eliciting inflammatory responses[4,5]; however, the enhanced viral replication and lung pathology observed in CA04-infected mice was not linked to dysregulated IL-17 production.

Cynomolgus macaques (*Macaca fascicularis*) have been used to study highly pathogenic avian H5N1 viruses[6,7] and the 1918 pandemic virus[8]. Infection of cynomolgus macaques with CA04 (see Methods for detailed procedures) resulted in a more prominent increase in body temperature than infection with KUTK-4 (Supplementary Fig. 6). This difference might originate from the observed differences in virus titres (Table 1 and Supplementary Table 2). No remarkable difference in body weight loss was found between the two groups (data not shown). CA04 replicated efficiently in the lungs and other respiratory organs of infected animals, similar to highly pathogenic influenza viruses[6,8] (Table 1). By contrast, conventional human influenza viruses are typically limited in their replicative ability in the lungs of infected primates[6,8] (Table 1), although a seasonal H1N1 virus was isolated from one animal on day 7 after infection. Pathological examination revealed that CA04 caused more severe lung lesions than did KUTK-4 (Fig. 1 and Supplementary Fig. 7). On day 3 after infection with CA04, alveolar spaces were occupied by oedematous exudate and inflammatory infiltrates (Fig. 1a, b); severe thickening of alveolar walls was also observed (Fig. 1b). Viral-antigen-positive cells were distributed in the inflammatory lesions, and many of these cells were elongated with thin cytoplasm and hemming around the alveolar wall, indicating type I pneumocytes (Fig. 1c). In addition to type I pneumocytes, CA04 viral antigens were also detected in considerable numbers of cuboidal, cytokeratin-positive cells, hence identified as type II pneumocytes (Fig. 1d and Supplementary Fig. 8), as has been reported for highly pathogenic avian H5N1 influenza viruses[6]. Upon infection with KUTK-4, large sections of infected lungs showed thickening of the alveolar wall on day 3 after infection (Fig. 1e). Although the infiltration of inflammatory cells was prominent at the alveolar wall (Fig. 1f), viral antigens were sparse and detected in type I (but not type II) pneumocytes (Fig. 1g). By contrast, the lungs of non-infected animals show clear alveolar spaces (Fig. 1h).

On day 7 after infection, lung pathology remained more severe for CA04- than for KUTK-4-infected lungs (Supplementary Fig. 7), although regenerative changes were seen for CA04. Nonetheless, considerable numbers of antigen-positive cells were still detectable (Supplementary Fig. 7c). Collectively, these findings demonstrate that CA04 causes more severe lung lesions in non-human primates than does a contemporary human influenza virus.

Induction of pro-inflammatory cytokines/chemokines in the lungs of CA04-infected macaques was variable at day 3 after infection (Supplementary Fig. 9). However, consistent with persisting lung pathology and inflammation on day 7 after infection, the levels of MCP-1, MIP-1α, IL-6 and IL-18 were markedly higher in the lungs of two of three CA04-infected macaques.

Ferrets are widely accepted as a suitable small-animal model for influenza virus pathogenicity and transmissibility studies. Infection of ferrets with S-OIVs or KUTK-4 did not cause marked changes in body temperature or weight in any group (data not shown). Although all test viruses were detected in nasal turbinates at similar titres on day 3 after infection (Supplementary Table 3), S-OIVs replicated to higher titres in trachea and lungs.

Pathological examination detected similar levels of viral antigen in the nasal mucosa of both CA04- and KUTK-4-infected ferrets (Supplementary Fig. 10a and e). However, the lungs of CA04-infected ferrets showed more severe bronchopneumonia with prominent viral antigen expression in the peribronchial glands and a few alveolar cells (Supplementary Fig. 10b–d) on day 3 after infection. By contrast, most of the lung appeared normal after infection with

Table 1 | Virus titres in organs of infected cynomolgus macaques

Organ	A/California/04/09 (H1N1)						A/Kawasaki/UTK-4/09 (H1N1)					
	Day 3 after infection			Day 7 after infection			Day 3 after infection			Day 7 after infection		
	1	2	3	4	5	6	7	8	9	10	11	12
Nasal mucosa	4.7	3.3	–	–	–	–	–	–	–	–	–	–
Oro/nasopharynx	6.3	4.4	4.7	–	7.9	–	–	–	4.3	–	–	4.8
Tonsil	6.4	–	–	–	7.1	–	–	–	2.8	–	–	3.0
Trachea	5.9	2.0	5.6	–	–	–	2.0	4.1	–	3.7	–	5.4
Bronchus (right)	5.7	2.9	4.3	–	5.1	–	–	2.5	–	3.5	–	3.8
Bronchus (left)	5.9	–	6.1	–	5.1	–	–	–	–	3.3	–	5.1
Lung (upper right)	5.7	5.6	4.5	–	–	–	2.7	–	–	–	–	–
Lung (middle right)	5.6	6.4	6.9	–	–	–	2.3	2.6	2.5	–	–	–
Lung (lower right)	6.1	4.5	6.0	–	–	–	2.6	2.6	–	–	–	3.4
Lung (upper left)	4.7	4.3	6.4	–	–	–	–	–	–	–	–	–
Lung (middle left)	5.8	4.3	6.3	–	–	–	–	–	–	–	–	–
Lung (lower left)	6.7	4.5	6.6	–	–	–	–	–	–	–	–	2.3
Conjunctiva	3.6	–	–	–	–	–	–	–	–	–	–	–

Cynomolgus macaques were inoculated with $10^{7.4}$ p.f.u. of virus (6.7 ml) through multiple routes (see Methods). Three macaques per group were killed on days 3 and 7 after infection for virus titration. No virus was recovered from lymph nodes (chest), heart, spleen, kidneys or liver of any of the animals. A dash indicates that virus was not detected (detection limit: 2 $\log_{10}$ p.f.u. g^{-1}). Numbers 1 to 12 indicate animal identification number. Values indicate virus titre (mean $\log_{10}$ p.f.u. g^{-1}).

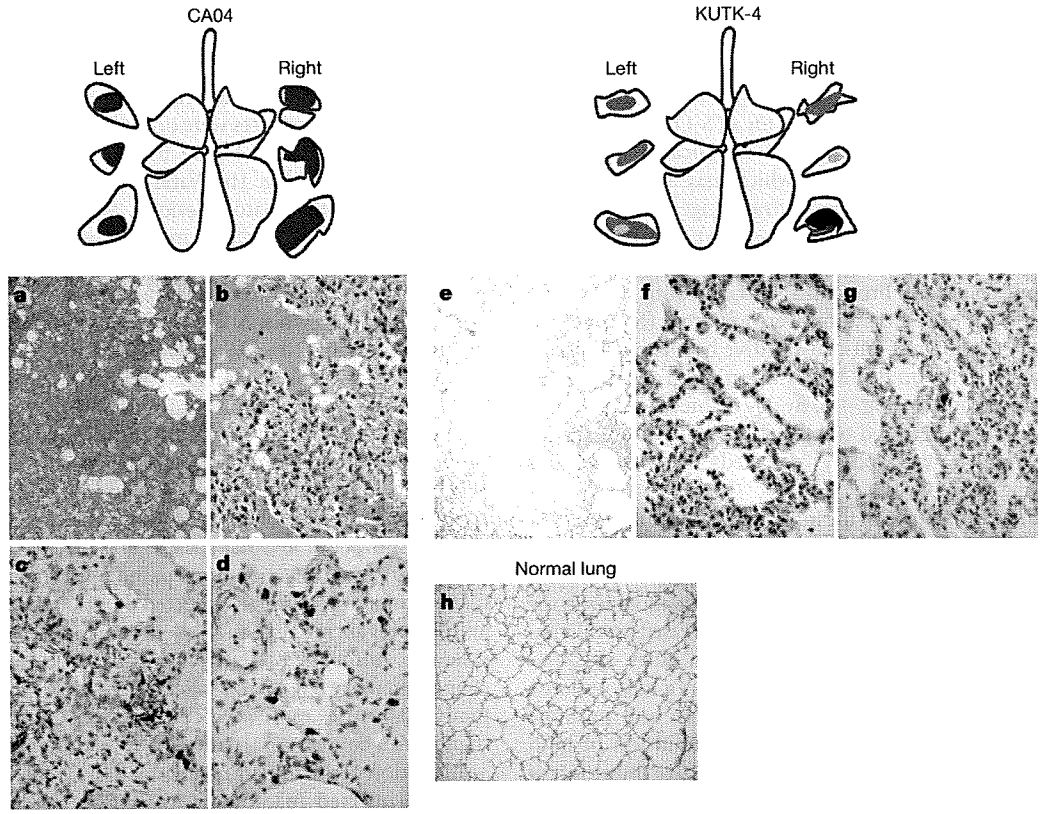

Figure 1 | Pathological examination of the lungs of infected cynomolgus macaques. a–h, Representative pathological images of CA04-infected (macaque no. 1, **a–d**), KUTK-4-infected (macaque no. 7, **e–g**) and mock-infected (**h**) lungs on day 3 after infection. One or two sections per lung lobe were examined. Representative findings are shown to depict the distribution of lesions in the sections (shown as cross-sections placed next to illustrations of each lung lobe), with or without viral antigen, as follows: brown, severe lung lesion containing moderate to many viral-antigen-positive cells; pink, mild lung lesions containing a few viral-antigen-positive cells; blue, lung lesions with alveolar wall thickening, with remaining air spaces unaffected. Original magnification: **a**, **e**, **h**, ×40; **b–d**, **f**, **g**, ×400.

KUTK-4 (Supplementary Fig. 10f and g). Thus, in all three mammalian models tested, CA04 seemed to be more pathogenic than a contemporary human H1N1 virus, KUTK-4.

Efficient human-to-human transmission is a critical feature of pandemic influenza viruses. To assess the transmissibility of CA04, naive ferrets in perforated cages were placed next to ferrets inoculated with 10^6 p.f.u. of CA04 (see Methods for detailed procedures). This experimental setting allows for aerosol transmission (that is, the exchange of respiratory droplets between the inoculated and non-inoculated ferrets) but prevents transmission by direct and indirect contact. All three contact ferrets were positive for CA04 virus on days 3 and 5 after infection (Supplementary Table 4). This transmission pattern is comparable to those of two human control influenza viruses that are known to transmit among ferrets: KUTK-4 and A/Victoria/3/75 (H3N2)[9]. By contrast, an avian influenza virus (A/duck/Alberta/35/76; H1N1) did not transmit (Supplementary Table 4).

Genetic analysis suggests that S-OIV originated in pigs[1]. However, there were no confirmed influenza virus outbreaks in Central American pigs before the reported S-OIV infections in humans. To assess S-OIV replication in pigs, we inoculated specific-pathogen-free miniature pigs, which are easier to manage, with CA04 or a classical swine influenza virus (A/swine/Hokkaido/2/81, H1N1). No signs of disease were observed (data not shown), although both viruses replicated efficiently in the respiratory organs of these animals (Supplementary Tables 5 and 6). Slightly higher titres of CA04 were detected in lungs on day 3 after infection, which is supported by pathological findings that show more apparent bronchitis and bronchiolitis in pigs infected with CA04 (Supplementary Fig. 11). The asymptomatic infection of CA04, despite efficient virus replication, might explain the lack of reports of S-OIV outbreaks in pigs before virus transmission to humans.

Antiviral compounds are the first line of defence against pandemic influenza viruses. Sequence analysis suggests that S-OIVs are resistant to ion channel inhibitors such as amantadine and rimantadine[1]. We therefore tested the licensed neuraminidase inhibitors oseltamivir and zanamivir, the experimental neuraminidase inhibitor R-125489 (the active form of CS-8958[10]) and the experimental compound T-705 (a broad-spectrum viral RNA polymerase inhibitor[11]) for their efficacy against CA04. In cell culture, CA04 was highly susceptible to all compounds tested (Supplementary Table 7), as were the human H1N1 control viruses A/Kawasaki/UTK-23/08 and KUTK-4, with the exception of the known oseltamivir resistance of KUTK-4. Comparable sensitivities were also found in an enzymatic neuraminidase inhibition assay[12] (Supplementary Table 8) and in mice (Fig. 2), consistent with observations in clinical settings.

A recent report suggested that 33% of individuals over 60 years of age had neutralizing antibodies to CA04 (http://www.cdc.gov/mmwr/preview/mmwrhtml/mm5819a1.htm; Morbidity and Mortality Weekly Report, Centers for Disease Control and Prevention), probably due to previous exposure to antigenically similar H1N1 viruses. In fact, both the human H1N1 viruses that circulated until 1957 and the classical swine virus HA gene of S-OIVs are descendants of the 1918 pandemic virus, possibly explaining their antigenic relatedness. In 1977, H1N1 viruses re-emerged that were genetically and antigenically very closely related to viruses circulating in the 1950s[13] and should thus have elicited neutralizing antibodies to CA04 among younger age groups; however, this does not seem to be the case, according to the above described report. To resolve this puzzling finding, we assessed the neutralizing activities of sera collected from a broad range of age groups against CA04 and KUTK-4. We used two sets of donor sera, collected in 1999 from residents and workers in a nursing home (donor set 1), and in April

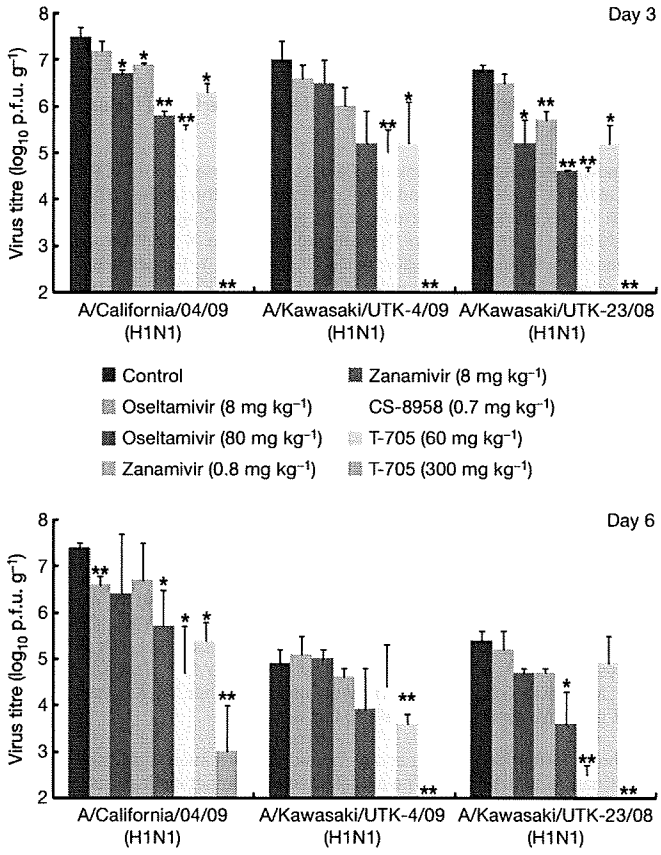

Figure 2 | CA04 sensitivity to antiviral compounds in mice. Mice were intranasally inoculated with 10^4 p.f.u. (50 µl) of CA04, KUTK-4 or A/Kawasaki/UTK-23/08 (H1N1). At 1 h after infection, mice were administered oseltamivir phosphate, zanamivir, CS-8958, T-705, or distilled water and PBS (control). Three mice per group were killed on days 3 and 6 after infection and the virus titres in lungs were determined by plaque assays in MDCK cells; results are reported as means ± s.d. The statistical significance of differences in lung virus titres of control mice and those treated with antivirals were assessed by use of the Student's *t*-test (asterisk, $P < 0.05$; double asterisk, $P < 0.01$).

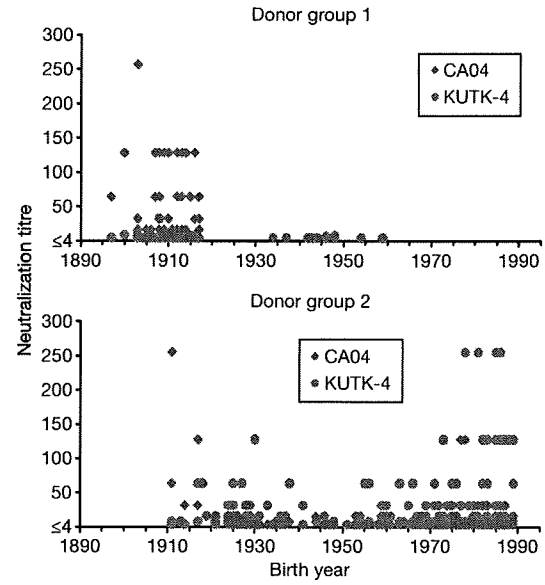

Figure 3 | Neutralization activities in human sera against viruses. Human sera of donor groups 1 (collected in 1999) and 2 (collected in April and May of 2009) were subjected to neutralization assays with CA04 and KUTK-4. Because the sera of donor group 1 were collected in 1999, little neutralization activity was expected against KUTK-4, which was isolated in 2009.

2009 from workers and patients in a hospital (donor set 2). High neutralizing activity against KUTK-4 was detected for many sera in donor set 2 (Fig. 3), but not for sera in donor set 1, probably because these sera were collected before the emergence of the current human H1N1 viruses. Interestingly, with few exceptions, no appreciable neutralizing antibodies against CA04 were found for individuals born after 1920; however, many of those born before 1918 had high neutralizing antibody titres (individual neutralizing antibody titres are shown in Supplementary Table 9). These data indicate that infection with the 1918 pandemic virus or closely related human H1N1 viruses, but not infection with antigenically divergent human H1N1 viruses circulating in the 1920s to 1950s, and again since 1977, elicited neutralizing antibodies to S-OIVs.

Our findings indicate that S-OIVs are more pathogenic in mammalian models than seasonal H1N1 influenza viruses. In fact, the ability of CA04 to replicate in the lungs of mice, ferrets and non-human primates, and to cause appreciable pathology in this organ, is reminiscent of infections with highly pathogenic H5N1 influenza viruses[14], as acknowledged in a recent report by the World Health Organization (http://www.who.int/wer/2009/wer8421/en/index.html). We therefore speculate that the high replicative ability of S-OIVs might contribute to a viral pneumonia characterized by diffuse alveolar damage that contributes to hospitalizations and fatal cases where no other underlying health issues exist (http://www.who.int/wer/2009/wer8421/en/index.html). In addition, sustained person-to-person transmission might result in the emergence of more pathogenic variants, as observed with the 1918 pandemic virus (reviewed in ref. 15). Furthermore, S-OIVs may acquire resistance to oseltamivir through mutations in their NA gene (as recently witnessed with human H1N1 viruses[16]), or through reassortment with co-circulating, oseltamivir-resistant seasonal human H1N1 viruses. Collectively, our findings are a reminder that S-OIVs have not yet garnered a place in history, but may still do so, as the pandemic caused by these viruses has the potential to produce a significant impact on human health and the global economy.

METHODS SUMMARY

Viruses and cells. All swine-origin H1N1 viruses were isolated and passaged in MDCK cells to produce viral stocks. The viruses and their passage histories are described in Methods. All experiments with S-OIVs were performed in approved enhanced biosafety level 3 (BSL3) containment laboratories.

MDCK cells and MDCK cells overexpressing the β-galactoside α2,6-sialyltransferase I gene[17] were maintained in Eagle's minimal essential medium (MEM) containing 5% newborn calf serum. Human airway epithelial (HAE) cells were obtained from residual surgical tissue trimmed from lungs during the process of transplantation. The bronchial specimens were dissected and enzymatically digested, and monolayers of HAE cells were isolated, cultured and differentiated as previously described[18].

Animals. Five- and six-week-old female BALB/c mice (Jackson Laboratory and Japan SLC Inc.), approximately three-to-four-year-old cynomolgus macaques (Ina Research Inc.), five-to-eight-month-old male ferrets (Marshall Farms and Triple F Farms) and two-month-old female specific-pathogen-free miniature pigs (Nippon Institute for Biological Science) were used according to approved protocols for the care and use of animals. Detailed procedures are provided in Methods.

Antiviral sensitivity of viruses in mice. Five-week-old female BALB/c mice (Japan SLC Inc.; groups of six) were anaesthetized with sevoflurane and intranasally inoculated with 10^4 p.f.u. (volume, 50 µl) of CA04, KUTK-4, or A/Kawasaki/UTK-23/08 (H1N1). At 1 h after infection, mice were administered antiviral compounds as described in detail in Methods. Three mice per group were killed on days 3 or 6 after infection and the virus titres in lungs were determined by plaque assays in MDCK cells.

Full Methods and any associated references are available in the online version of the paper at www.nature.com/nature.

Received 2 June; accepted 3 July 2009.
Published online 13 July 2009.

1. Novel Swine-Origin Influenza A (H1N1) Virus Investigation Team. Emergence of a novel swine-origin influenza A (H1N1) virus in humans. *N. Engl. J. Med.* 360, 2605–2615 (2009).

2. Kawaoka, Y. & Webster, R. G. Sequence requirements for cleavage activation of influenza virus hemagglutinin expressed in mammalian cells. *Proc. Natl Acad. Sci. USA* **85**, 324–328 (1988).
3. Hatta, M., Gao, P., Halfmann, P. & Kawaoka, Y. Molecular basis for high virulence of Hong Kong H5N1 influenza A viruses. *Science* **293**, 1840–1842 (2001).
4. Iwakura, Y., Nakae, S., Saijo, S. & Ishigame, H. The roles of IL-17A in inflammatory immune responses and host defense against pathogens. *Immunol. Rev.* **226**, 57–79 (2008).
5. Hamada, H. *et al.* Tc17, a unique subset of CD8 T cells that can protect against lethal influenza challenge. *J. Immunol.* **182**, 3469–3481 (2009).
6. Baskin, C. R. *et al.* Early and sustained innate immune response defines pathology and death in nonhuman primates infected by highly pathogenic influenza virus. *Proc. Natl Acad. Sci. USA* **106**, 3455–3460 (2009).
7. Rimmelzwaan, G. F. *et al.* Pathogenesis of influenza A (H5N1) virus infection in a primate model. *J. Virol.* **75**, 6687–6691 (2001).
8. Kobasa, D. *et al.* Aberrant innate immune response in lethal infection of macaques with the 1918 influenza virus. *Nature* **445**, 319–323 (2007).
9. Maines, T. R. *et al.* Lack of transmission of H5N1 avian-human reassortant influenza viruses in a ferret model. *Proc. Natl Acad. Sci. USA* **103**, 12121–12126 (2006).
10. Yamashita, M. *et al.* CS-8958, a prodrug of the new neuraminidase inhibitor R-125489, shows long-acting anti-influenza virus activity. *Antimicrob. Agents Chemother.* **53**, 186–192 (2009).
11. Furuta, Y. *et al. In vitro* and *in vivo* activities of anti-influenza virus compound T-705. *Antimicrob. Agents Chemother.* **46**, 977–981 (2002).
12. Hayden, F. G. *et al.* Inhaled zanamivir for the prevention of influenza in families. Zanamivir Family Study Group. *N. Engl. J. Med.* **343**, 1282–1289 (2000).
13. Nakajima, K., Desselberger, U. & Palese, P. Recent human influenza A (H1N1) viruses are closely related genetically to strains isolated in 1950. *Nature* **274**, 334–339 (1978).
14. Peiris, J. S. *et al.* Re-emergence of fatal human influenza A subtype H5N1 disease. *Lancet* **363**, 617–619 (2004).
15. Wright, P. F., Neumann, G. & Kawaoka, Y. *Fields Virology* (eds Knipe, D. M. *et al.*) 1691–1740 (Wolters Kluwer/Lippincott Williams & Wilkins, 2007).
16. Moscona, A. Global transmission of oseltamivir-resistant influenza. *N. Engl. J. Med.* **360**, 953–956 (2009).
17. Hatakeyama, S. *et al.* Enhanced expression of an α2,6-linked sialic acid on MDCK cells improves isolation of human influenza viruses and evaluation of their sensitivity to a neuraminidase inhibitor. *J. Clin. Microbiol.* **43**, 4139–4146 (2005).
18. Jakiela, B., Brockman-Schneider, R., Amineva, S., Lee, W. M. & Gern, J. E. Basal cells of differentiated bronchial epithelium are more susceptible to rhinovirus infection. *Am. J. Respir. Cell Mol. Biol.* **38**, 517–523 (2008).

Supplementary Information is linked to the online version of the paper at www.nature.com/nature.

Acknowledgements We thank the Centers for Disease Control (CDC) for A/California/04/09 virus and R. Fouchier for A/Netherlands/603/09 virus. We thank K. Wells for editing the manuscript, and M. McGregor, R. Moritz, A. Hanson, H. Ishida, H. Tsuchiya, R. Torii, N. Yamamoto, K. Soda, N. Nomura and H. Yoshida for technical assistance. We also thank T. Umemura, Y. Sunden and T. Tanaka for pathological analyses of virus-infected pigs. This work was supported by National Institute of Allergy and Infectious Diseases Public Health Service research grants, by an NIAID-funded Center for Research on Influenza Pathogenesis (CRIP, HHSN266200700010C), by Grant-in-Aid for Specially Promoted Research, by a contract research fund for the Program of Founding Research Centers for Emerging and Reemerging Infectious Diseases from the Ministry of Education, Culture, Sports, Science and Technology, and by grants-in-aid from the Ministry of Health and by ERATO (Japan Science and Technology Agency).

Author Contributions Y.I., K.S., M.K., T.W., Y.S., M.H., Y.M., D.T., Y.S.-T., T.N., M. Imai, S.W., K.I.-H., T.H., N.S., H.K., K.O. and Y.K. designed the experiments; Y.I., K.S., M.K., T.W., Y.S., M.H., D.T., Y.S.-T., T.N., S.S., M. Imai, Y.H., S.W., C.L., S.Y., K.F., S.M., H. Imai, S.K., M. Ito, R.T., K.I.-H., M.S., T.H., Kei Takahashi, A.M., H. Ishigaki, M. Nakayama, M. Okamatsu, Kazuo Takahashi, D.W., P.A.S., R.S., H.S., Y.F., M. Yamashita, K.M., K.N., M. Nakamura, R.B.-S., J.G., H.M. and M. Yamazaki performed the experiments; Y.I., K.S., M.K., T.W., Y.S., M.H., Y.M., Y.S.-T., T.N., M. Imai, S.W., C.L., S.Y., K.I.-H., T.H., H.G., M.S., M. Ozawa, G.N., H.K., K.O. and Y.K. analysed data; Y.I., K.S., M.K., T.W., Y.S., M.H., Y.M., Y.S.-T., T.N., M. Imai, K.I.-H., M.S., M. Ozawa, G.N., K.O. and Y.K. wrote the manuscript. Y.I., K.S., M.K., T.W., Y.S., M.H. and Y.M. contributed equally to this work.

Author Information Reprints and permissions information is available at www.nature.com/reprints. The authors declare competing financial interests: details accompany the full-text HTML version of the paper at www.nature.com/nature. Correspondence and requests for materials should be addressed to Y.K. (kawaokay@svm.vetmed.wisc.edu).

METHODS

Viruses. A/California/04/09 (H1N1; CA04) was provided by the Centers for Disease Control (CDC). A/Wisconsin/WSLH049/09 (H1N1) was isolated from a patient with mild symptoms, whereas A/Wisconsin/WSLH34939/09 (H1N1) was isolated from a hospitalized patient. A/Netherlands/603/09 (H1N1) was isolated from a patient with mild symptoms and was provided by R. Fouchier. A/Osaka/164/09 (H1N1) was also isolated from a patient with mild symptoms.

The following influenza viruses served as controls: A/Kawasaki/UTK-4/09 (H1N1; KUTK-4; passaged twice in MDCK cells), an oseltamivir-resistant seasonal human virus; A/WSN/33 (H1N1; generated by reverse genetics and passaged twice in MDCK cells), a typical spherical influenza virus[19]; A/Kawasaki/UTK-23/08 (H1N1; passaged twice in MDCK cells), an oseltamivir-sensitive seasonal human virus; A/Victoria/3/75 (H3N2; passaged several times in eggs after it was obtained from the CDC), a human virus; A/swine/Hokkaido/2/81 (H1N1; passaged several times in eggs), a classical swine virus; and A/duck/Alberta/35/76 (H1N1; passaged several times in eggs), an avian virus. All experiments with S-OIV viruses were performed in enhanced biosafety level 3 (BSL3) containment laboratories at the University of Wisconsin-Madison, which are approved for such use by the CDC and the US Department of Agriculture, or in BSL3 containment laboratories at the University of Tokyo, the Shiga University of Medical Science, or the Hokkaido University, all of which are approved for such use by the Ministry of Agriculture, Forestry and Fisheries, Japan.

Viral pathogenesis in mice. Six-week-old female BALB/c mice (Jackson Laboratory and Japan SLS Inc.) were used in this study. Baseline body weights were measured before infection. Three mice per group were anaesthetized with isoflurane and intranasally inoculated with 10^2, 10^3, 10^4, or 10^5 p.f.u. (50 μl) of CA04 and KUTK-4, or undiluted virus from virus stocks (CA04, $10^{6.5}$ p.f.u.; KUTK-4, $10^{6.6}$ p.f.u.). Body weight and survival were monitored daily for 14 days and mice with body weight loss of more than 25% of pre-infection values were killed. For virological and pathological examinations, 6 mice per group were intranasally infected with 10^5 p.f.u. of S-OIVs and KUTK-4 and 3 mice per group were killed on days 3 and 6 after infection. The virus titres in various organs were determined by plaque assays in MDCK cells.

Growth kinetics of virus in human airway epithelial (HAE) cells. Cultures of differentiated HAE cells were washed extensively with PBS to remove accumulated mucus and infected with virus at a multiplicity of infection (MOI) of 0.001 from the apical surface. The inoculum was removed after 1 h of incubation at 35 °C, and cells were further incubated at 35 °C. Samples were collected at 12, 24, 48, 72 and 96 h after infection from the apical surface. Apical harvesting was performed by adding 500 μl of medium to the apical surface, followed by incubation for 30 min at 35 °C, and removal of the medium from the apical surface. The titres of viruses released into the cell culture supernatant were determined by plaque assay in MDCK cells.

Experimental infection of cynomolgus macaques. Approximately three-to-four-year-old cynomolgus macaques (*Macaca fascicularis*) from the Philippines (obtained from Ina Research Inc.), weighing 2.1–3.0 kg and serologically negative by AniGen AIV antibody ELISA, which detects all influenza A virus subtypes (Animal Genetics Inc.), were used in this study. Baseline body weights were established by two or three measurements before infection. Under anaesthesia, telemetry probes (TA10CTA-D70, Data Sciences International) were implanted in the peritoneal cavities of animals to monitor body temperature. Six macaques per group were intramuscularly anaesthetized with ketamine (5 mg per kg) and xylazine (1 mg per kg) and inoculated with a suspension containing $10^{6.5}$ p.f.u. ml^{-1} of CA04 or KUTK-4 virus through a combination of intratracheal (4.5 ml), intranasal (0.5 ml per nostril), ocular (0.1 ml per eye) and oral (1 ml) routes (resulting in a total infectious dose of $10^{7.4}$ p.f.u.). Macaques were monitored every 15 min for changes in body temperature. On days 1, 3, 5 and 7 after infection, nasal and tracheal swabs and bronchial brush samples were collected. On days 3 and 7 after infection, 3 macaques per group were killed for virological and pathological examinations. The virus titres in various organs and swabs were determined by plaque assays in MDCK cells. Experiments were carried out in accordance with the Guidelines for the Husbandry and Management of Laboratory Animals of the Research Center for Animal Life Science at Shiga University of Medical Science, Shiga, Japan, and approved by the Shiga University of Medical Science Animal Experiment Committee and Biosafety Committee.

Experimental infection of ferrets. We used five-to-eight-month-old male ferrets (Marshall Farms and Triple F Farms), which were serologically negative by haemagglutination inhibition (HI) assay for currently circulating human influenza viruses. Baseline body temperatures and body weights were established by one or two measurements before infection. Six ferrets per group were intramuscularly anaesthetized with ketamine and xylazine (5 mg and 0.5 mg per kg of body weight, respectively) and intranasally inoculated with 10^6 p.f.u. (500 μl) of S-OIVs or KUTK-4. On days 3 and 6 after infection, 3 ferrets per group were killed for virological and pathological examinations. The virus titres in various organs were determined by plaque assays in MDCK cells.

Experimental infection of miniature pigs. Two-month-old female specific-pathogen-free miniature pigs (Nippon Institute for Biological Science), which were serologically negative by AniGen AIV antibody ELISA for currently circulating influenza viruses, were used in this study. Baseline body temperatures were measured once before infection. Four pigs per group were intranasally inoculated with $10^{6.2}$ p.f.u. (1 ml) of viruses. Nasal swabs were collected daily. On day 3 after infection, two pigs per group were killed and their tissues collected for examination. On day 14 after infection, the remaining two pigs per group were killed for virological and pathological examinations. Virus titres in various organs and swabs were determined by plaque assays in MDCK cells. The miniature pigs used in this study were housed in self-contained isolator units (Tokiwa Kagaku) at a BSL3 facility and experiments were conducted in accordance with guidelines established by the Animal Experiment Committee of the Graduate School of Veterinary Medicine, Hokkaido University, Japan.

Pathological examination. Excised tissues of the nasal turbinates, trachea and/or lungs of killed mice, macaques, ferrets and pigs were preserved in 10% phosphate-buffered formalin. Tissues were then processed for paraffin embedding and cut into 5-μm-thick sections. One section from each tissue sample was stained using a standard haematoxylin-and-eosin procedure, whereas another one was processed for immunohistological staining with an anti-influenza virus rabbit antibody (R309; prepared in our laboratory) that reacts comparably with CA04 and KUTK-4. Specific antigen–antibody reactions were visualized by 3,3′-diaminobenzidine tetrahydrochloride staining using a Dako EnVision system (Dako Co. Ltd).

Ferret transmission study. For transmission studies in ferrets, animals were housed in adjacent transmission cages that prevent direct and indirect contact between animals but allow spread of influenza virus through the air. Three or two 5-to-8-month-old ferrets were intranasally inoculated with 10^6 p.f.u. (500 μl) of CA04, KUTK-4, A/Victoria/3/75 (H3N2) or A/duck/Alberta/35/76 (H1N1) (inoculated ferrets). One day after infection, three or two naive ferrets were each placed in a cage adjacent to an inoculated ferret (contact ferrets). All ferrets were monitored daily for changes in body temperature and weight, and the presence of clinical signs. To assess viral replication in the upper respiratory tract, viral titres were determined in nasal washes collected from virus-inoculated and contact ferrets on day 1 after inoculation or co-housing, respectively, and then every other day (up to 9 days).

Cytokine and chemokine measurement. For cytokine and chemokine measurement, homogenates of mouse lungs were processed with the Bio-Plex Mouse Cytokine 23-Plex and 9-Plex panels (Bio-Rad Laboratories), whereas macaque lung homogenates were measured with the MILLIPLEX MAP Non-human Primate Cytokine/Chemokine Panel–Premixed 23-Plex (Millipore). Array analysis was performed by Bio-Plex Protein Array system (Bio-Rad Laboratories).

Antiviral sensitivity of viruses in mice. To test the antiviral sensitivity of viruses in mice, animals were infected as described in the Methods Summary section and 1 h later administered the following antiviral compounds: (1) oseltamivir phosphate: 8 or 80 mg per kg per 400 μl (divided into two oral administrations per day) for 5 days; (2) zanamivir: 0.8 or 8 mg per kg per 50 μl in one daily intranasal administration for 5 days; (3) CS-8958: 0.7 mg per kg per 50 μl in one intranasal administration; (4) T-705: 60 or 300 mg per kg per 400 μl (divided into two oral administrations per day) for 5 days; (5) or distilled water orally (200 μl) and PBS intranasally (50 μl). Three mice per group were killed on day 3 or 6 after infection and the virus titres in lungs were determined by plaque assays in MDCK cells.

Sensitivity to antiviral compounds in tissue culture. MDCK cells overexpressing the β-galactoside α2,6-sialyltransferase I gene (or, for studies with T-705, regular MDCK cells) were infected with CA04, KUTK-4, or A/Kawasaki/UTK-23/08 (H1N1) at a multiplicity of infection of 0.001. After incubation for 1 h at 37 °C, growth medium containing various concentrations of oseltamivir carboxylate (the active form of oseltamivir), zanamivir, R-125489 (the active form of CS-8958), or T-705 was added to the cells. Twenty-four hours later, the culture supernatants were harvested and the 50% tissue-culture infectious dose ($TCID_{50}$) in MDCK cells determined. On the basis of the $TCID_{50}$ value, the 90% inhibitory concentration (IC_{90}) was calculated.

Neuraminidase inhibition assay. To assess the sensitivity of viruses to neuraminidase inhibitors (that is, oseltamivir, zanamivir and CS-8958), neuraminidase inhibition assays were performed as described previously[20]. Briefly, diluted viruses were mixed with various concentrations of oseltamivir carboxylate, zanamivir, or R-125489 in 2-(*N*-morpholino)ethanesulphonic acid containing calcium chloride, and incubated for 30 min at 37 °C. Then, we added methylumbelliferyl-*N*-acetylneuraminic acid (Sigma) as a fluorescent substrate to this mixture. After incubation for 1 h at 37 °C, sodium hydroxide in 80% ethanol was added to the mixture to stop the reaction. The fluorescence of the solution was measured at an

excitation wavelength of 360 nm and an emission wavelength of 465 nm and the 50% inhibitory concentration (IC_{50}) was calculated.

Neutralization assay with human sera. Human sera were collected in 1999 or 2009 from donor group 1 (age range: 50–112 years as of 2009, mean = 92.7 ± 15.0 years) or 2 (age range: 20–68 years as of 2009, mean = 48.2 ± 23.7 years), respectively. These sera were treated with receptor-destroying enzyme (DENKA SEIKEN CO.) to remove inhibitors of influenza virus replication. One hundred $TCID_{50}$ (50% tissue culture infectious dose) of CA04 and KUTK-4 were pre-incubated with twofold serial dilutions of treated sera, incubated for 60 min on MDCK cells, which were then observed for cytopathic effects to determine the neutralizing activity of the test sera. Our research protocol was approved by the Research Ethics Review Committee of the Institute of Medical Science, the University of Tokyo (approval numbers: 21-6-0428 for donor group 1; 21-7-0529 for donor group 2).

Immunofluorescence microscopy. MDCK cells were infected with CA04, KUTK-4, or WSN and fixed with 4% paraformaldehyde 16–24 h later. Infected cells were incubated with the following primary antibodies: mouse anti-HA (7B1b), anti-HA (IVC102), or mouse anti-HA (WS3-54) antibody against CA04, KUTK-4 or WSN, respectively. Cells were then incubated with Alexa Fluor 488 goat anti-mouse immunoglobulin G (Invitrogen), and examined with a confocal laser-scanning microscope (LSM510META; Carl Zeiss).

Electron microscopy. MDCK cells were infected with CA04, KUTK-4 or WSN at a multiplicity of infection of 10. At 16–24 h after infection, cells were processed for ultrathin section electron microscopy and scanning electron microscopy as described previously[19,21].

19. Noda, T. *et al.* Architecture of ribonucleoprotein complexes in influenza A virus particles. *Nature* **439**, 490–492 (2006).
20. Kiso, M. *et al.* Resistant influenza A viruses in children treated with oseltamivir: descriptive study. *Lancet* **364**, 759–765 (2004).
21. Neumann, G. *et al.* Ebola virus VP40 late domains are not essential for viral replication in cell culture. *J. Virol.* **79**, 10300–10307 (2005).

Analytical Biochemistry 389 (2009) 80–82

Contents lists available at ScienceDirect

Analytical Biochemistry

journal homepage: www.elsevier.com/locate/yabio

Notes & Tips

Application of retrovirus-mediated expression cloning for receptor screening of a parasite

Kyousuke Kobayashi [a], Kentaro Kato [a,*], Tatsuki Sugi [a], Daisuke Yamane [a], Masayuki Shimojima [b], Yukinobu Tohya [a], Hiroomi Akashi [a]

[a] Department of Veterinary Microbiology, Graduate School of Agricultural and Life Sciences, University of Tokyo, Bunkyo-ku, Tokyo 113-8657, Japan
[b] Division of Virology, Department of Microbiology and Immunology, Institute of Medical Science, University of Tokyo, Minato-ku, Tokyo 108-8639, Japan

ARTICLE INFO

Article history:
Received 7 February 2009
Available online 12 March 2009

ABSTRACT

Retrovirus-mediated expression cloning has been applied in both virology and cell biology. Although there is some difficulty in applying this technique to screening for a receptor recognized by an intracellular parasite, we modified the conventional method to identify a putative receptor for the *Plasmodium falciparum* BAEBL protein. We show that this method is effective in screening for a parasite receptor.

To develop effective means of preventing and treating infectious diseases, it is important to understand the interactions between a pathogen and its host. For a pathogen to invade host cells, such as viruses or protozoans, the pathogen must recognize a receptor on the surface of the host cells.

Various methods have been developed for identifying the partner that interacts with a particular molecule. One such method is retrovirus-mediated expression cloning [1–3], which has been applied to studies in both virology [4,5] and cell biology [6]. We sought to apply this method to screen for the receptor recognized by an intracellular apicomplexan parasite.

Shimojima and coworkers [4] identified CD134 as the primary receptor for feline immunodeficiency virus (FIV)[1] using the following procedure. First, a complementary DNA (cDNA) library made from the FIV-sensitive cell line MYA-1 was transduced to the FIV-insensitive cell line P3S63Ag8U.1 (P3U1) using a retrovirus vector. As a result, a proportion of the P3U1 cells expressed the receptor. To isolate the receptor-expressing cells, the transduced P3U1 cells were panned using a dish coated with FIV particles. The receptor molecule was determined from the sequence of feline CD134 cDNA amplified by polymerase chain reaction (PCR) using genomic DNA from an isolated cell clone as the template and vector-specific primers.

This procedure has two problems before it can be applied to a parasite. One problem is the antigen used to coat the dish. In the case of a virus, virions are effective antigens because a virus has relatively simple entry pathways mediated by a few surface molecules and the virion is soluble. By contrast, in the case of a parasite such as *Plasmodium falciparum*, which has multiple invasion pathways mediated by many ligands, an intact parasite itself cannot be used as the coating antigen. To solve this problem, we made a recombinant protein of interest fused with the Fc region of murine immunoglobulin G2a (mIgG2aFc). This protein can be coated on the bottom of a dish via an anti-mouse IgG Fc antibody.

The other problem is the criterion for selecting cells as the source of the cDNA library and target cells for an expression retrovirus cDNA library. For example, because the host cells of *P. falciparum* are erythrocytes that lack a nucleus, the construction of a cDNA library seems impossible. By contrast, because *Toxoplasma gondii* is thought to infect a broad host range of cells, it should be difficult to find cells that lack a receptor recognized by a *T. gondii* ligand. We attempted the following strategy to overcome this problem. The binding affinities between various cell types and the recombinant protein prepared as the coating were tested using flow cytometry. Cells with potent affinity were judged to have a receptor, whereas cells with weak or no affinity were judged to lack a receptor. Therefore, the former can serve as the source of the cDNA library and the latter can serve as target cells.

The procedure used in our modified method for screening for a parasite invasion receptor is shown in Fig. 1. To confirm whether this method works, we searched for a receptor for the *P. falciparum* protein BAEBL, which belongs to the Duffy binding-like family and is associated with erythrocyte invasion. Using a baculovirus expression system, region II of BAEBL, which is a critical region for binding, was expressed as a recombinant protein, designated BAEBL/Fc, fused with mIgG2aFc at the N terminal and an octa-histidine tag at the C terminal (Kobayashi et al., unpublished data). Similarly, a recombinant protein of the Fc region, designated

* Corresponding author. Fax: +81 3 5841 8184.
E-mail address: akkato@mail.ecc.u-tokyo.ac.jp (K. Kato).

[1] *Abbreviations used:* FIV, feline immunodeficiency virus; cDNA, complementary DNA; P3U1, P3S63Ag8U.1; PCR, polymerase chain reaction; mIgG2aFc, Fc region of murine immunoglobulin G2a; Tn5, BTI-Tn-5B1-4; Ni–NTA, nickel–nitrilotriacetic acid; mRNA, messenger RNA; MLV, Moloney murine leukemia virus; PBS, phosphate-buffered saline; 2FCS–PBS, PBS containing 2% fetal calf serum.

0003-2697/$ - see front matter © 2009 Elsevier Inc. All rights reserved.
doi:10.1016/j.ab.2009.03.008

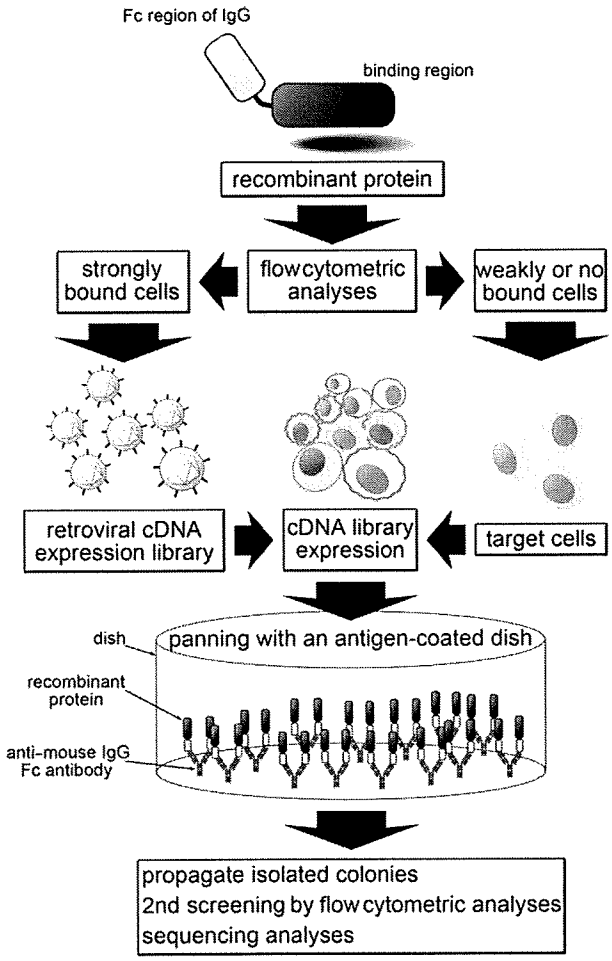

Fig. 1. Flow diagram of retrovirus-mediated expression cloning of a receptor recognized by a parasite. An Fc fusion protein containing the binding region of a molecule of interest is examined by testing its binding affinity to several cell lines. A retroviral cDNA library is constructed using mRNA extracted from cells showing strong binding affinity. Cells showing weak or no affinity are infected with a retrovirus stock carrying the cDNA library and then added to a dish coated with the recombinant protein and panned to isolate adhesive colonies. The colonies are subjected to flow cytometry to confirm the ligand binding. The cDNA sequences extracted from the confirmed cells are then analyzed.

mIgG2aFc, was prepared as a negative control. These proteins secreted from *Trichoplusia ni* BTI-Tn-5B1-4 (Tn5) insect cells were purified on nickel–nitrilotriacetic acid (Ni–NTA) agarose for flow cytometric analysis.

Next, we assessed the binding ability of BAEBL/Fc to several cell lines, including COS7, NIH3T3, P3U1, CrFK, FL74, 293T, Jurkat, and K562 cells, using flow cytometry. The cells (1×10^5) were resuspended in 27 nM purified recombinant protein solution and incubated for 1 h at 4 °C. The binding of the recombinant protein was detected using an anti-mouse IgG antibody labeled with fluorescein isothiocyanate, as described previously [4], and was quantified using FACSCalibur (Becton Dickinson, San Jose, CA, USA) and WinMDI 2.9 software. BAEBL/Fc showed relatively strong affinity for 293T human kidney cells and showed relatively weak affinity for Jurkat human T-cells (Fig. 2A and B), suggesting that 293T cells express a receptor for BAEBL.

A cDNA library was constructed using a previously described method [4,5] with several modifications. The cDNA library was generated from poly(A)+ messenger RNA (mRNA) purified from 293T cells and cloned into pMX. The cDNA library was packed into Moloney murine leukemia virus (MLV) particles by transfection into Plat-E cells and used to transduce Jurkat–EcoVRc cells. These are MLV-sensitive Jurkat cells that express the mouse cationic amino acid transporter and are prepared using a self-inactivating human immunodeficiency virus vector [7].

A dish was incubated at 4 °C overnight with 10 μg/ml goat anti-mouse IgG Fc (Rockland, Gilbertsville, PA, USA) in 4 ml of phosphate-buffered saline (PBS), rinsed in PBS containing 2% fetal calf serum (2FCS–PBS), and then incubated at room temperature for 30 min in 2FCS–PBS. The culture supernatant (10 ml) from Tn5 cells expressing BAEBL/Fc was added to the dish and incubated at room temperature for 30 min. The medium was replaced twice. The coated protein was fixed by incubating the dish in culture supernatant containing 1% paraformaldehyde at room temperature for 30 min. The dish was then washed five times in 2FCS–PBS before adding 1×10^7 transduced Jurkat–EcoVRc cells suspended in 4 ml of 2FCS–PBS. The cells were incubated at 37 °C for 2 h. Nonadherent cells were removed by washing. Adherent cells were cultured for 6 days, with a second wash on day 3. The adherent cells that formed colonies were suspended by pipetting in a penicillin cup and were transferred to a new culture plate. After propagating each clone, the reactivity of BAEBL against each clone was reconfirmed using flow cytometry. We obtained a clone, designated BJT6, to which BAEBL/Fc binds strongly (Fig. 2C). Genomic DNA from BJT6 was isolated and subjected to PCR amplification using KOD plus polymerase (Toyobo, Osaka, Japan) and the pMX primers [8]. Following amplification, this clone yielded a specific cDNA fragment encoding the full-length open reading frame of human glypican 1.

To confirm that glypican 1 really contributes to BAEBL binding, we evaluated the difference in the affinity of BAEBL/Fc to cells with or without glypican 1. Human glypican 1 cDNA was cloned into the *Bam*HI/*Sal*I sites of pMX to produce pMX–glypican 1. Jurkat–glypican 1 and Jurkat–mock cells were produced by the transfection of pMX–glypican 1 and pMX vectors, respectively, into Plat-E cells using Lipofectamine 2000 (Invitrogen, Carlsbad, CA, USA). Jurkat–EcoVRc cells were incubated with the culture supernatant from the transfected Plat-E cells and were analyzed 2 to 4 days postinfection. The flow cytometric analysis indicated that BAEBL/Fc showed greater affinity for Jurkat–glypican 1 than for Jurkat–mock (Fig. 2D and E), indicating that glypican 1 enhances the binding of BAEBL to the cell surface. This suggested that heparan sulfate proteoglycans, such as glypican 1, function to promote BAEBL binding and merozoite invasion, as seen in further analyses (Kobayashi et al., unpublished data). As shown here, this modified receptor screening strategy is applicable to parasite studies and has potential to increase our understanding of parasites.

Acknowledgments

This study was supported by a Grant-in-Aid for Young Scientists from the Ministry of Education, Culture, Sports, Science, and Technology (MEXT) of Japan and the Bio-oriented Technology Research Advancement Institution (BRAIN).

References

[1] T. Kitamura, M. Onishi, S. Kinoshita, A. Shibuya, A. Miyajima, G.P. Nolan, Efficient screening of retroviral cDNA expression libraries, Proc. Natl. Acad. Sci. USA 92 (1995) 9146–9150.
[2] M. Onishi, S. Kinoshita, Y. Morikawa, A. Shibuya, J. Phillips, L.L. Lanier, D.M. Gorman, G.P. Nolan, A. Miyajima, T. Kitamura, Applications of retrovirus-mediated expression cloning, Exp. Hematol. 24 (1996) 324–329.
[3] M. Shimojima, T. Miyazawa, Y. Sakurai, Y. Nishimura, Y. Tohya, Y. Matsuura, H. Akashi, Usage of myeloma and panning in retrovirus-mediated expression cloning, Anal. Biochem. 315 (2003) 138–140.
[4] M. Shimojima, T. Miyazawa, Y. Ikeda, E.L. McMonagle, H. Haining, H. Akashi, Y. Takeuchi, M.J. Hosie, B.J. Willett, Use of CD134 as a primary receptor by the feline immunodeficiency virus, Science 303 (2004) 1192–1195.
[5] A. Makino, M. Shimojima, T. Miyazawa, K. Kato, Y. Tohya, H. Akashi, Junctional adhesion molecule 1 is a functional receptor for feline calicivirus, J. Virol. 80 (2006) 4482–4490.

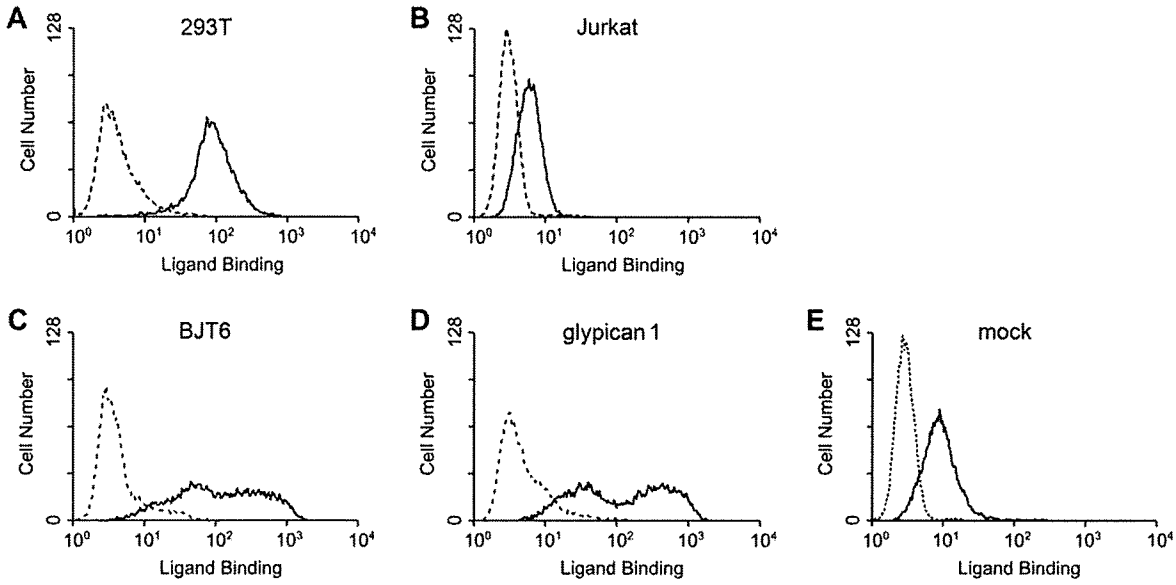

Fig. 2. Detection of recombinant protein binding using flow cytometry. The affinity of BAEBL/Fc (solid line) compared with mIgG2aFc (broken line) was determined for several cell lines. BAEBL/Fc bound strongly to 293T cells (A) and relatively poorly to Jurkat cells (B). The BJT6 clone was isolated as a result of the expression cloning (C). Jurkat-EcoVRc cells transduced with a retrovirus vector carrying cDNA of glypican 1 (D) or an empty plasmid (E) were incubated with BAEBL/Fc (solid line) or mIgG2aFc (broken line). Protein binding was detected and quantified as described in the text.

[6] T. Kitamura, Y. Koshino, F. Shibata, T. Oki, H. Nakajima, T. Nosaka, H. Kumagai, Retrovirus-mediated gene transfer and expression cloning: powerful tools in functional genomics, Exp. Hematol. 31 (2003) 1007–1014.

[7] M. Shimojima, Y. Ikeda, Y. Kawaoka, The mechanism of Axl-mediated Ebola virus infection, J. Infect. Dis. 196 (Suppl. 2) (2007) S259–S263.

[8] T. Kitamura, Y. Morikawa, Isolation of T-cell antigens by retrovirus-mediated expression cloning, Methods Mol. Biol. 134 (2000) 143–152.

JOURNAL OF VIROLOGY, May 2009, p. 4153–4162 Vol. 83, No. 9
0022-538X/09/$08.00+0 doi:10.1128/JVI.02642-08

Mutational Analysis of Conserved Amino Acids in the Influenza A Virus Nucleoprotein▽†

Zejun Li,[1] Tokiko Watanabe,[1] Masato Hatta,[1] Shinji Watanabe,[1] Asuka Nanbo,[1] Makoto Ozawa,[2] Satoshi Kakugawa,[2] Masayuki Shimojima,[2] Shinya Yamada,[2] Gabriele Neumann,[1] and Yoshihiro Kawaoka[1,2,3,4]*

Department of Pathobiological Sciences, School of Veterinary Medicine, University of Wisconsin—Madison, 2015 Linden Drive, Madison, Wisconsin 53706[1]; Division of Virology, Department of Microbiology and Immunology,[2] and International Research Center for Infectious Diseases, Institute of Medical Science,[3] University of Tokyo, Tokyo 108-8639, Japan; and ERATO Infection-Induced Host Responses Project, Japan Science and Technology Agency, Saitama 332-0012, Japan[4]

Received 22 December 2008/Accepted 10 February 2009

The nucleoprotein (NP), which has multiple functions during the virus life cycle, possesses regions that are highly conserved among influenza A, B, and C viruses. To better understand the roles of highly conserved NP amino acids in viral replication, we conducted a comprehensive mutational analysis. Using reverse genetics, we attempted to generate 74 viruses possessing mutations at conserved amino acids of NP. Of these, 48 mutant viruses were successfully rescued; 26 mutants were not viable, suggesting a critical role of the respective NP amino acids in viral replication. To identify the step(s) in the viral life cycle that is impaired by these NP mutations, we examined viral-genome replication/transcription, NP localization, and incorporation of viral-RNA segments into progeny virions. We identified 15 amino acid substitutions in NP that inhibited viral-genome replication and/or transcription, resulting in significant growth defects of viruses possessing these substitutions. We also found several NP mutations that affected the efficient incorporation of multiple viral-RNA (vRNA) segments into progeny virions even though a single vRNA segment was incorporated efficiently. The respective conserved amino acids in NP may thus be critical for the assembly and/or incorporation of sets of eight vRNA segments.

Influenza A virus consists of eight negative-sense single-stranded viral genomic-RNA segments and encodes at least 11 proteins (reviewed in reference 39). These genomic RNAs are incorporated into virions as ribonucleoprotein (RNP) complexes, which consist of the viral RNA (vRNA) associated with three viral polymerase subunit proteins (PA, PB1, and PB2) and nucleoprotein (NP). Upon binding to cell surface receptors, virions are internalized by receptor-mediated endocytosis. After fusion of the viral and endosomal membranes, the viral RNPs (vRNPs) are released into the cytoplasm and transported to the nucleus, where viral-genome replication and transcription take place (34). Newly synthesized vRNAs are associated with the NP and form vRNPs in the nucleus (4). Subsequently, the vRNPs are transported to the cytoplasm and packaged into the progeny virus particles, which then bud from the cells.

NP, a basic protein composed of 498 amino acids, is a major component of vRNPs (reviewed in reference 33). It contains an RNA-binding region at its N terminus (residues 1 to 181) (1, 19) and two domains, responsible for NP-NP self-interaction, at residues 189 to 358 and 371 to 465 (8) (Fig. 1A). Both of these NP functions are important to maintain the organization of vRNPs. Besides its structural role, NP is involved in many other functions throughout the virus replication cycle. In the early stages of the viral life cycle, NP facilitates vRNP import into the nucleus via its two nuclear localization signals (NLSs), an unconventional NLS (residues 3 to 13) and a bipartite NLS (residues 198 to 216) (35). NP also plays a role in RNA synthesis in the nucleus (15). It is required for the synthesis of longer RNAs, although three polymerase proteins are sufficient to synthesize short RNAs (14). NP also interacts with the viral polymerase proteins PB1 and PB2 (3), suggesting a potential role in the regulation of polymerase activity. Export of vRNPs from the nucleus to the cytoplasm is promoted via an interaction between NP and M1/NS2 (2, 22, 27, 29, 38, 40, 42). NP has an important role in RNP export; besides binding to the M1 protein, NP contains a cytoplasmic accumulation signal (residues 327 to 345), which interacts with F actin and causes cytoplasmic retention of NP late in infection (2, 5). In addition, NP contains a nuclear export signal that is recognized by the nuclear export receptor CRM1 (9). Overexpression of CRM1 biases transfected NP toward cytoplasmic accumulation, and the two proteins interact in in vitro binding assays (9).

The NP possesses regions that are highly conserved among influenza A, B, and C viruses (23). Mena et al. (23) used mutational analysis to identify several amino acid residues that are important for vRNA replication in the conserved regions of NP. For most of the conserved amino acids, however, the biological significance and the role in the viral life cycle remain unknown. To close this gap in knowledge, we attempted to generate 74 mutant viruses possessing mutations at conserved

* Corresponding author. Mailing address: Department of Pathobiological Sciences, School of Veterinary Medicine, University of Wisconsin—Madison, 2015 Linden Drive, Madison, WI 53706. Phone: (608) 265-4925. Fax: (608) 265-5622. E-mail: kawaokay@svm.vetmed.wisc.edu.

† Supplemental material for this article may be found at http://jvi.asm.org/.

▽ Published ahead of print on 18 February 2009.

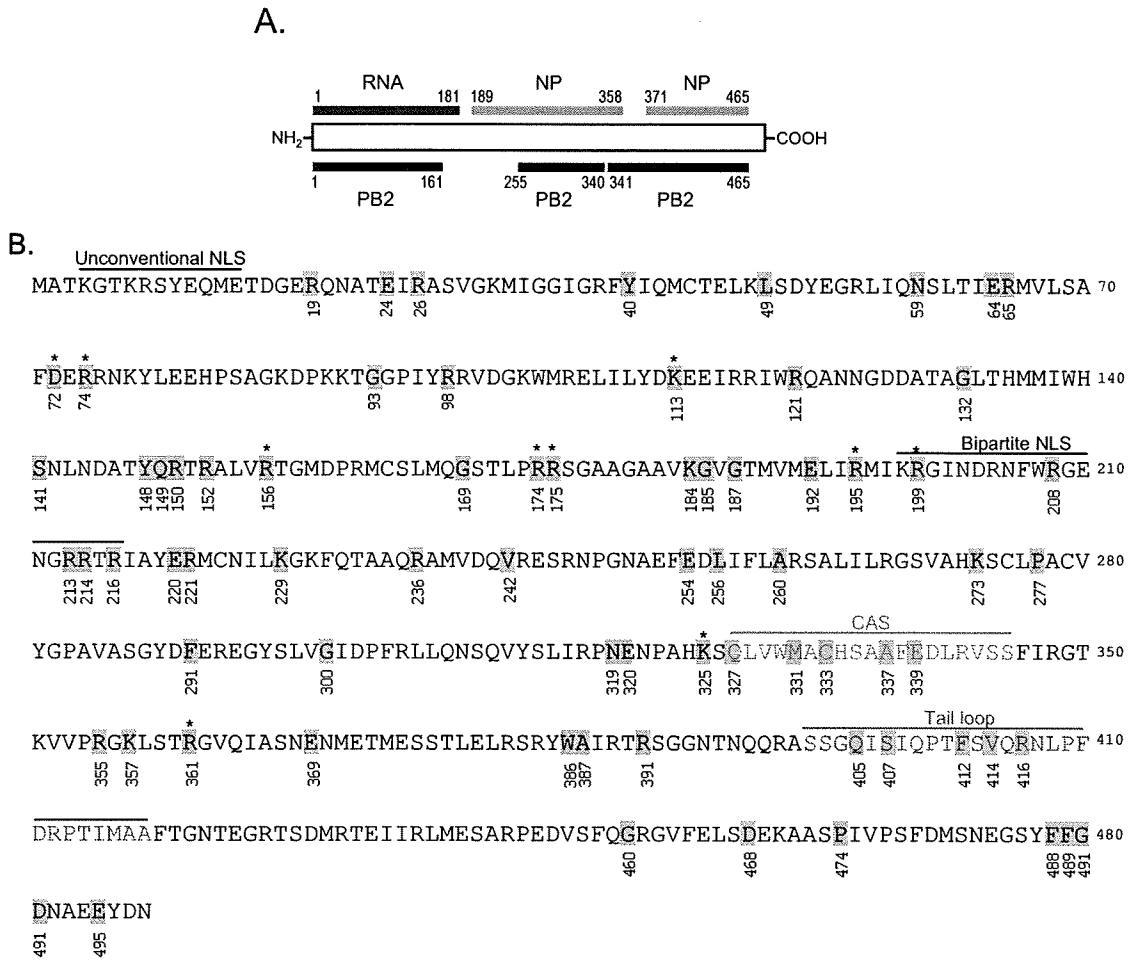

FIG. 1. Individual residues targeted by mutagenesis. (A) The NP regions responsible for binding to RNA (red), NP itself (orange), and PB2 (purple) are shown. (B) Amino acid sequence of WSN NP. Amino acids tested in this study are shaded. The unconventional NLS, the bipartite NLS, the cytoplasmic accumulation signal (CAS), and the NP tail loop, which mediates NP oligomerization, are shown in different colors. NP mutants flagged with an asterisk were further tested for intracellular localization and incorporation efficiency of a vRNA segment(s) into VLPs, in addition to replicative ability and polymerase activity.

residues of NP, and for the mutations that did not support viral growth, we studied the steps at which the mutations negatively affected NP functions.

MATERIALS AND METHODS

Cells. 293T cells were maintained in Dulbecco's modified Eagle medium supplemented with 10% fetal calf serum. Madin-Darby canine kidney (MDCK) cells were maintained in minimum essential medium containing 5% newborn calf serum. NP-expressing MDCK (MDCK-NP) cells were maintained in minimum essential medium containing 5% newborn calf serum and 5 μg/ml puromycin. All cells were maintained at 37°C in 5% CO_2.

MDCK-NP cells stably expressing NP from A/WSN/33 (H1N1; WSN) were established by infecting MDCK cells with retroviruses that were generated by cotransfecting 293T cells with the murine leukemia virus retroviral vector pMX (30) containing the NP gene, the internal ribosome entry site (IRES) sequence, and the puromycin resistance gene (designated pMX-WSNNP-IRES-puro [see below]) and plasmids expressing Gal/Pol, NF-κB, and vesicular stomatitis virus G protein (17), which were kind gifts from Bill Sugden (University of Wisconsin—Madison). A stable MDCK cell clone expressing NP was selected in medium containing 0.15 mg/ml puromycin (Roche, Mannheim, Germany) by indirect immunostaining with a monoclonal antibody to NP.

Plasmid construction. The NP segment of WSN virus was reverse transcribed with an oligonucleotide complementary to the conserved 3′ end of the vRNA (16) and a pair of NP gene-specific oligonucleotide primers containing BsmBI sites. The PCR product was cloned into the pT7Blueblunt vector (Novagen, Madison, WI), and the resultant plasmid was referred to as pT7-WSN-NP. After digestion with BsmBI, the fragment containing the NP gene was cloned into the BsmBI sites of the pHH21 vector, which contains the human RNA polymerase I promoter and the mouse RNA polymerase I terminator separated by BsmBI sites (24), resulting in the generation of pPolI-NP (all plasmids derived from pHH21 for the expression of vRNA are referred to as PolI constructs in this report).

pCAGGs/MCS-NP, for the expression of the NP protein, was generated by inserting the BsmBI-digested NP fragment into the BsmBI sites of a modified pCAGGS/MCS (18, 25) vector. The substitution mutations listed in Table 1 were first introduced into the pT7-WSN-NP plasmid by in vitro site-directed mutagenesis (Stratagene, La Jolla, CA) and then subcloned into the pHH21 and pCAGGS/MCS vectors by using the unique BsmBI restriction enzyme sites. All mutations were verified by sequencing.

pPolI-WSN-NA-*firefly*-luciferase produces a virus-like RNA in which the coding region for firefly luciferase is flanked by the packaging signals of the NA segment (12). This plasmid was generated by inserting the firefly luciferase open reading frame between the BamHI and XhoI sites of pPolI-WSN-NA-MCS, which was constructed by modifying the start codon of pPolINA(183)GFP(157) (12) (in essence, we replaced ATATG at nucleotide positions 113 to 117 and 161 to 165 with GCGCG) and by replacing the sequence from the initiation of the enhanced green fluorescent protein (GFP) gene to the StuI site on pPolI-WSN-NA(183)GFP(157). pPolI-HA-GFP, for the generation of a virus-like RNA encoding GFP, was generated as described previously (36).

pCAGGS-*Renilla*, for the expression of *Renilla* luciferase, was generated by

TABLE 1. Phenotypic analyses of mutant NP proteins

NP[a]	Virus rescue[b]	Mean virus titer at 48 h postinfection (log_{10} PFU/ml) ±SD[c]		Group[d]	Relative luciferase activity at 48 h posttransfection (%)[e]	
		33°C	37°C		33°C	37°C
Wild type	+	7.99 ± 0.01	8.85 ± 0.07	I	100.00 ± 6.88	100.00 ± 13.51
R19A	+	7.28 ± 0.02	9.00 ± 0.00	I	94.68 ± 4.14	88.26 ± 1.30
E24A	+	6.65 ± 0.05	8.67 ± 0.05	I	131.38 ± 14.44	95.84 ± 4.20
Y40A	+	7.98 ± 0.05	8.41 ± 0.01	I	91.83 ± 4.06	81.73 ± 5.45
L49A	+	8.12 ± 0.01	8.54 ± 0.07	I	151.00 ± 7.27	142.78 ± 8.76
R65A	+	6.29 ± 0.07	8.49 ± 0.02	I	138.46 ± 3.43	108.60 ± 17.82
R98A	+	8.30 ± 0.01	8.55 ± 0.06	I	108.01 ± 1.14	89.65 ± 3.67
R121A	+	6.37 ± 0.20	7.94 ± 0.02	I	144.83 ± 4.15	104.00 ± 2.76
G132A	+	7.62 ± 0.05	9.11 ± 0.02	I	145.46 ± 10.02	106.67 ± 4.86
S141A	+	8.09 ± 0.01	8.87 ± 0.05	I	133.72 ± 2.09	100.26 ± 3.02
Q149A	+	3.65 ± 0.01	7.51 ± 0.16	I	135.63 ± 6.60	102.19 ± 2.52
G169A	+	7.89 ± 0.03	8.43 ± 0.21	I	126.76 ± 2.21	94.92 ± 3.96
K184A	+	6.40 ± 0.08	7.68 ± 0.02	I	145.34 ± 11.35	96.27 ± 5.72
G185A	+	6.58 ± 0.16	7.46 ± 0.06	I	153.55 ± 6.32	95.09 ± 4.86
G187A	+	6.31 ± 0.23	8.43 ± 0.01	I	114.82 ± 5.33	99.31 ± 1.40
R214A	+	7.21 ± 0.01	8.01 ± 0.07	I	122.85 ± 4.95	87.02 ± 14.18
R216A	+	6.32 ± 0.06	6.92 ± 0.04	I	111.38 ± 4.64	85.36 ± 6.68
E220A	+	5.22 ± 0.06	8.57 ± 0.19	I	62.84 ± 3.39	103.46 ± 8.18
K229A	+	6.92 ± 0.01	8.03 ± 0.09	I	113.40 ± 0.68	97.47 ± 5.12
R236A	+	5.07 ± 0.05	7.61 ± 0.00	I	107.59 ± 2.69	90.13 ± 14.06
V242A	+	7.67 ± 0.13	8.15 ± 0.11	I	136.01 ± 4.81	101.33 ± 2.46
L256A	+	6.33 ± 0.10	6.97 ± 0.07	I	143.86 ± 3.42	87.44 ± 1.70
P277A	+	8.31 ± 0.01	8.79 ± 0.03	I	131.35 ± 3.02	98.03 ± 2.96
F291A	+	7.15 ± 0.05	8.41 ± 0.01	I	126.04 ± 3.53	89.44 ± 5.27
G300A	+	5.02 ± 0.06	7.75 ± 0.01	I	100.10 ± 3.52	86.88 ± 3.82
N319A	+	7.75 ± 0.11	8.36 ± 0.05	I	107.45 ± 2.23	81.28 ± 4.23
Q327A	+	6.74 ± 0.09	7.19 ± 0.27	I	125.66 ± 0.88	95.25 ± 7.13
C333A	+	8.06 ± 0.05	8.9 ± 0.01	I	105.19 ± 4.78	99.49 ± 6.63
K357A	+	7.78 ± 0.01	8.7 ± 0.08	I	105.22 ± 0.25	81.12 ± 1.17
E369A	+	7.27 ± 0.21	7.98 ± 0.02	I	114.80 ± 4.74	142.64 ± 1.72
W386A	+	5.44 ± 0.11	7.53 ± 0.05	I	88.39 ± 4.83	125.05 ± 8.59
G460A	+	6.68 ± 0.06	8.88 ± 0.04	I	118.59 ± 17.56	138.93 ± 10.31
P474A	+	6.04 ± 0.03	8.79 ± 0.08	I	115.52 ± 3.98	116.35 ± 3.24
G490A	+	7.63 ± 0.04	8.86 ± 0.13	I	113.78 ± 11.54	104.90 ± 6.71
E495A	+	7.21 ± 0.09	8.3 ± 0.02	I	73.02 ± 1.39	83.08 ± 7.90
R26A	+	1.54 ± 0.09	3.81 ± 0.03	II	79.44 ± 0.71	85.62 ± 1.65
*R74A	+	3.11 ± 0.09	4.42 ± 0.08	II	139.73 ± 9.61	109.25 ± 2.07
*R175A	+	2.91 ± 0.01	4.11 ± 0.05	II	170.32 ± 5.96	108.56 ± 6.54
E192A	+	4.16 ± 0.02	6.03 ± 0.01	II	78.03 ± 3.16	82.87 ± 1.66
R221A	+	4.56 ± 0.03	4.75 ± 0.13	II	111.94 ± 4.57	93.17 ± 4.51
M331A	+	1.00 ± 0.00	4.77 ± 0.1	II	99.45 ± 8.38	83.98 ± 7.56
R391A	+	2.89 ± 0.03	6.57 ± 0.02	II	70.66 ± 2.04	63.56 ± 0.46
S407A	+	1.00 ± 0.00	6.19 ± 0.03	II	5.40 ± 0.39	86.15 ± 0.28
V414A	+	1.69 ± 0.12	6.85 ± 0.06	II	47.29 ± 6.11	92.27 ± 1.14
D468A	+	3.54 ± 0.34	6.67 ± 0.10	II	97.46 ± 2.33	81.45 ± 5.87
D491A	+	5.09 ± 0.07	5.82 ± 0.09	II	52.09 ± 0.67	73.18 ± 4.46
N59A	+	ND	ND	III	159.52 ± 4.80	54.32 ± 1.72
E64A	+	ND	ND	III	193.40 ± 14.30	0.03 ± 0.00
E320A	+	ND	ND	III	145.78 ± 6.37	51.05 ± 1.47
*D72A	−	ND	ND	IV	121.17 ± 1.30	135.07 ± 1.05
G93A	−	ND	ND	IV	131.30 ± 10.53	55.13 ± 2.74
*K113A	−	ND	ND	IV	183.46 ± 12.21	106.16 ± 5.07
Y148A	−	ND	ND	IV	100.87 ± 3.15	82.89 ± 10.15
R150A	−	ND	ND	IV	12.46 ± 0.79	32.17 ± 1.44
R152A	−	ND	ND	IV	100.52 ± 1.78	77.61 ± 14.19
*R156A	−	ND	ND	IV	123.85 ± 6.03	95.24 ± 3.16
*R174A	−	ND	ND	IV	214.89 ± 17.15	100.56 ± 6.91
*R195A	−	ND	ND	IV	160.59 ± 14.23	105.41 ± 5.63
*R199A	−	ND	ND	IV	152.91 ± 10.97	102.41 ± 6.38
R208A	−	ND	ND	IV	0.19 ± 0.01	0.13 ± 0.01
R213A	−	ND	ND	IV	32.42 ± 0.36	38.29 ± 7.36
E254A	−	ND	ND	IV	0.26 ± 0.03	0.37 ± 0.13
A260R	−	ND	ND	IV	0.04 ± 0.00	0.02 ± 0.01
K273A	−	ND	ND	IV	0.19 ± 0.02	0.04 ± 0.01
*K325A	−	ND	ND	IV	157.38 ± 7.37	134.67 ± 12.73

Continued on following page

TABLE 1—*Continued*

NP[a]	Virus rescue[b]	Mean virus titer at 48 h postinfection (log_{10} PFU/ml) ±SD[c]		Group[d]	Relative luciferase activity at 48 h posttransfection (%)[e]	
		33°C	37°C		33°C	37°C
A337R	−	ND	ND	IV	0.16 ± 0.00	0.03 ± 0.00
E339A	−	ND	ND	IV	0.16 ± 0.01	0.03 ± 0.01
R355A	−	ND	ND	IV	52.91 ± 0.47	45.07 ± 1.06
*R361A	−	ND	ND	IV	105.57 ± 0.49	104.60 ± 20.58
A387R	−	ND	ND	IV	0.15 ± 0.00	0.04 ± 0.00
Q405A	−	ND	ND	IV	0.16 ± 0.01	0.05 ± 0.01
F412A	−	ND	ND	IV	0.40 ± 0.32	0.03 ± 0.00
R416A	−	ND	ND	IV	0.21 ± 0.10	0.03 ± 0.00
F488A	−	ND	ND	IV	0.20 ± 0.01	8.05 ± 1.02
F489A	−	ND	ND	IV	0.16 ± 0.01	0.23 ± 0.22

[a] We selected 74 amino acids that are conserved among influenza A, B, and C virus NPs for mutagenesis. NP mutants flagged with an asterisk were further tested for intracellular localization, and incorporation efficiency of a vRNA segment(s) into VLPs, in addition to replicative ability and polymerase activity.

[b] Viruses were generated using an established plasmid-based reverse-genetics system. +, NP mutant virus recovery was verified by plaque assay, cytopathic effect, and NP gene sequencing; −, no replicating virus was recovered.

[c] MDCK cells were infected with wild-type WSN or NP mutant virus at an MOI of 0.0001. At 48 h postinfection, the culture supernatants were harvested and subjected to plaque assays in MDCK cells. ND, plaques were not detected.

[d] Based on virus rescue and viral-replication properties, NP mutants were categorized into four groups. Group I, at either 33°C or 37°C, viruses were attenuated by less than 2 log units; group II, mutant viruses were attenuated by more than 2 log units at both temperatures tested; group III, NP mutant viruses were rescued but did not form plaques at 48 h postinfection; group IV, NP mutant virus were not rescued.

[e] The abilities of mutant NPs to support vRNA replication/transcription in an in vitro assay were examined in 293T cells as described in Materials and Methods. Since luciferase levels reflect the overall transcription and replication activity of the polymerase complex, we defined the polymerase activity levels as high, normal, and low for mutants that exhibited >120%, 80% to 120%, and <80%, respectively, of the wild-type activity.

inserting the open reading frame of the *Renilla* luciferase gene into the BsmBI sites of pCAGGs/MCS.

The pPolI-NP(Met$^-$) plasmid, used to generate vRNA that did not encode NP due to the lack of a start codon, was generated by changing the 1st through the 7th ATG codons to TAG and by changing the 14th and 15th ATG codons to TAG and TGA, respectively, using in vitro site-directed mutagenesis (Stratagene, La Jolla, CA).

The plasmid pMX-WSNNP-IRES-puro was constructed as follows. First, the puromycin resistance gene was inserted into XbaI and SalI sites of the plasmid pIRES (Clontech, Mountain View, CA), and then a fragment containing the IRES sequence and the puromycin resistance gene was inserted into EcoRI and SalI sites of the pMX retroviral vector (30). This plasmid was designated pMX-IRES-puro. Finally, the WSN NP gene was cloned into EcoRI and MluI sites of pMX-IRES-puro.

Plasmid-driven reverse genetics. All viruses used in this study were generated by reverse genetics, using plasmids expressing the eight vRNA segments, the three polymerase proteins, and NP, as described by Neumann et al. (24). At 48 h posttransfection, viruses were harvested and used to inoculate MDCK cells for the production of stock viruses. The NP genes of transfectant viruses were sequenced to confirm the origins of the genes and the presence of the intended mutations and to ensure that no unwanted mutations were present.

Virus-like particles (VLPs) were generated from 293T cells transfected with eight PolI constructs producing eight vRNA segments [i.e., PB1, PB2, PA, NA, M, NS, HA-GFP, and NP(Met$^-$), which lacks a start codon] and five protein expression constructs producing PB1, PB2, PA, hemagglutinin (HA), and mutant or wild-type NP (see Fig. 3). These plasmids were mixed with transfection reagent (2 μl of Trans IT LT-1 [Mirus, Madison, WI] per μg of DNA), incubated at room temperature for 20 min, and added to 10^6 293T cells. Six hours later, the DNA transfection reagent mixture was replaced by 1 ml Opti-MEM (Invitrogen, Grand Island, NY). Forty-eight hours after transfection, the supernatant was harvested, treated with trypsin, and used to determine the number of VLPs containing the test genes, as described below.

Replicative properties of viruses. MDCK cells were infected with wild-type WSN or NP mutant virus at a multiplicity of infection (MOI) of 0.0001 at 33°C and 37°C, respectively. At 48 h postinfection, the culture supernatants were collected and subjected to plaque assays in MDCK cells for virus titration.

Luciferase assay. 293T cells were transfected with plasmids for the expression of the viral proteins PA, PB1, PB2, and NP (wild-type or mutated NP) and pPolI-WSN-NA-*firefly*-luciferase. Plasmid pCAGGS-*Renilla* was used as an internal control for the dual-luciferase assay. As a negative control, 293T cells were transfected with the same plasmids, with the exception of the NP expression plasmid. After transfection, the cells were incubated at 33°C or 37°C for 48 h, and then luciferase activity was measured with a dual-luciferase reporter system (Promega, Madison, WI) on a Glomax microplate luminometer (Promega, Madison, WI) according to the manufacturer's instructions.

Immunostaining assay. MDCK cells were transfected with pCAGGs/MCS plasmids expressing wild-type or mutant NP. At 9 h and 24 h posttransfection, the cells were fixed and indirect immunofluorescence assays were performed. Briefly, the cells were washed twice with phosphate-buffered saline (PBS), fixed with 3.7% paraformaldehyde (in PBS) for 20 min at room temperature, washed again, and permeabilized with 0.5% Triton X-100 for 10 min. After being blocked with 10% bovine serum albumin for 20 min at room temperature, the cells were incubated with an anti-NP monoclonal antibody (347/3) for 30 min. The cells were then incubated with fluorescein isothiocyanate-labeled goat anti-mouse antibody immunoglobulin G (1:200 dilution; Roche) for 30 min, washed, and mounted with 10 mM *p*-phenylenediamine in glycerol-PBS (9:1), pH 8.5. To avoid the detection of newly synthesized NP, protein synthesis was inhibited by adding cycloheximide (50 mg/ml; Sigma) to the growth medium at 9 h posttransfection. Twenty-four hours later, indirect immunofluorescence assays were performed. Samples were observed under a fluorescence microscope or a confocal laser microscope (LSM510META; Carl Zeiss, Jena, Germany).

Determination of the number of VLPs. To determine the number of VLPs containing at least one vRNA (i.e., HA-GFP vRNA), culture supernatants of 293T cells transfected with plasmids for VLP production (as described above) were used to infect MDCK cells. To provide polymerase and NP that supported HA-GFP vRNA replication and transcription, cells were coinfected with WSN virus at an MOI of 0.1 (see Fig. 3). Sixteen hours postinfection, the infected cells were fixed, and the cells expressing GFP were counted under a fluorescence microscope.

To determine the number of VLPs containing a set of four vRNAs (i.e., PB1, PB2, PA, and HA-GFP vRNAs), the culture supernatants of transfected cells were used to infect MDCK-NP cells that stably expressed WSN NP (see Fig. 3). GFP expression from the HA-GFP vRNA would occur only if VLPs contained the HA-GFP vRNA together with the PB2, PB1, and PA vRNAs. GFP-positive cells, therefore, represented VLPs that possessed at least the PB2, PB1, PA, and HA-GFP vRNAs. As described above, the number of GFP-expressing cells was determined at 16 h postinfection.

RESULTS

Generation of NP mutant viruses. For mutagenesis, we selected amino acids that are highly conserved among influenza A, B, and C viruses, as well as amino acids that may be critical for RNA binding, as suggested by the recently published crystal

structure of influenza A virus NP (41). In total, 74 amino acid residues were selected for testing (Fig. 1B). Using plasmid-driven reverse genetics (24), we were able to generate 48 mutant viruses (Table 1). The remaining 26 mutant viruses were not viable (Table 1), suggesting that the respective mutations in NP are critical for the viral life cycle.

Replicative properties of NP mutant viruses. For all viable mutant viruses, we next examined their replicative abilities in cell culture. Briefly, MDCK cells were infected with wild-type WSN or NP mutant viruses at an MOI of 0.0001 and incubated at 33°C and 37°C. Forty-eight hours later, the culture supernatants were harvested and subjected to plaque assays in MDCK cells for virus titration. Based on their abilities to support viral replication, the NP mutants could be divided into four groups. As shown in Table 1, groups I, II, and III include all 48 recovered NP mutant viruses, while group IV contains the 26 nonviable mutant viruses.

Group I contains 34 mutant viruses whose titers were less than 2 log units lower than that of wild-type WSN virus at either 33°C or 37°C. Seventeen viruses (possessing NP mutations R19A, Y40A, L49A, R98A, G132A, S141A, G169A, R214A, V242A, P277A, F291A, N319A, C333A, K357A, E369A, G490A, and E495A) were attenuated by less than 1 log unit at both 33°C and 37°C. Mutant viruses Q149A, K184A, G185A, R216A, R236A, L256A, G300A, Q327A, and W386A were clearly attenuated at both 33°C and 37°C, with virus titers reduced by more than 1 log unit compared to wild-type WSN virus, whereas E24A, R65A, R121A, G187A, E220A, K229A, G460A, and P474A were attenuated only at 33°C. Of these viruses, mutants Q149A, E220A, R236A, G300A, and W386A were attenuated by more than 2.5 log units at 33°C. The NP sequences of these mutant viruses were reconfirmed, and one unexpected mutation was found at position 140 (His to Arg) in the NP protein of mutant R65A (the significance of this substitution is currently unknown).

The NP mutant viruses in group II were significantly attenuated, i.e., their titers were more than 2 log units lower than that of wild-type WSN virus at both 33°C and 37°C. Eleven NP mutant viruses (R26A, R74A, R175A, E192A, R221A, M331A, R391A, S407A, V414A, D468A, and D491A) comprised this group. The titers of four mutants (R26A, R74A, R175A, and M331A) were more than 4 log units lower than that of wild-type WSN virus at both 33°C and 37°C. Four other viruses (R391A, S407A, V414 A, and D468A) were attenuated by more than 4 log units at 33°C but only 2 to 3 log units at 37°C.

Group III contains three mutant viruses, N59A, E64A, and E320A, which were unable to form plaques, although cytopathic effects were observed in MDCK cells infected with these mutants. The 50% tissue culture infective doses of N59A, E64A, and E320A were 5.5, 3.5, and 6.5 $\log_{10}$ 50% tissue culture infective doses/ml at 33°C, respectively.

Group IV includes the 26 nonviable mutants (D72A, G93A, K113A, Y148A, R150A, R152A, R156A, R174A, R195A, R199A, R208A, R213A, E254A, A260R, K273R, K325A, A337R, E339R, R355A, R361A, R387A, Q405A, F412A, R416A, F488A, and F489A), attesting to a critical role of these amino acids in the viral life cycle.

Polymerase activities of replication complexes containing NP mutants. As stated above and shown in Table 1, we identified NP amino acid substitutions that caused viral growth defects. To assess the effects of these substitutions on vRNA transcription activity, we tested the activities of NP mutants by using a minireplicon system. pPolI-WSN-NA-*firefly*-luciferase synthesizes a modified influenza virus NA vRNA in which the coding region for firefly luciferase replaces the native NA coding sequences. The luciferase levels thus reflect the overall transcription and replication activities of the polymerase complex upon cotransfection of cells with pPolI-WSN-NA-*firefly*-luciferase and plasmids for the expression of the viral PA, PB1, PB2, and NP (wild-type or mutant NP), which support both replication and transcription from a vRNA template (32). At 48 h posttransfection, luciferase activity was measured. We found that NP mutants in group I, whose mutations had no or moderate effects on virus replicative ability, had at least 80% and 60% of the luciferase activity of wild-type NP at 37°C and 33°C, respectively (Table 1). NP mutant E220A showed reduced activity to support polymerase function at 33°C but not at 37°C. Other mutants in group I (i.e., Q149A, R236A, and G300A) showed no defect in supporting polymerase function compared to wild-type NP at 33°C, even though the respective virus titers were more than 2 log units lower than that of wild-type WSN virus at 33°C. Hence, these NP mutations do not affect genome replication and transcription, but other steps in the viral life cycle.

In group II, six NP mutants, R26A, E192A, R391A, S407A, V414A, and D491A, showed lower activity to support polymerase function at 33°C than wild-type NP, suggesting that these mutations may cause virus attenuation at low temperatures. Interestingly, R74A and R175A showed normal activity to support polymerase function at 37°C, and even higher activity at 33°C, compared to wild-type NP, whereas the respective viruses were attenuated by more than 4 log units. These results suggest that these mutations may inhibit steps other than genome replication and transcription, such as transport, assembly, and/or virion incorporation.

Mutants in group III showed some temperature sensitivity, expressing more than 145% of wild-type luciferase activity at 33°C but less than 55% at 37°C. Specifically, mutant E64A lost the ability to support reporter gene transcription at 37°C but expressed 193% of wild-type luciferase activity at 33°C. Notably, these mutant viruses could not form plaques at either 33°C or 37°C, even though they expressed higher luciferase activity than wild-type WSN virus at 33°C.

In group IV, many of the variants (i.e., R150A, R208A, R213A, E254A, A260R, K273A, A337R, E339A, R355A, A387R, Q405A, F412A, R416A, F488A, and F489A) showed no or very low luciferase activity at both 33°C and 37°C. Hence, these mutations likely lost the ability to support viral polymerase activity, resulting in the growth defect of the mutant viruses (Table 1). The remaining mutants expressed reasonable levels of luciferase activity at either 33°C or 37°C. Of these mutants, D72A, K113A, R156A, R174A, R195A, R199A, K325A, and R361A showed normal or high polymerase activity at both 33°C and 37°C despite the observed failure of virus rescue (Table 1). These data suggest a role of the respective amino acids in processes such as intracellular transport, assembly, and/or packaging.

Localization of mutant NPs. We found that 10 NP variants (D72A, R74A, K113A, R156A, R174A, R175A, R195A, R199A, K325A, and R361A) caused viral growth defects with no ap-

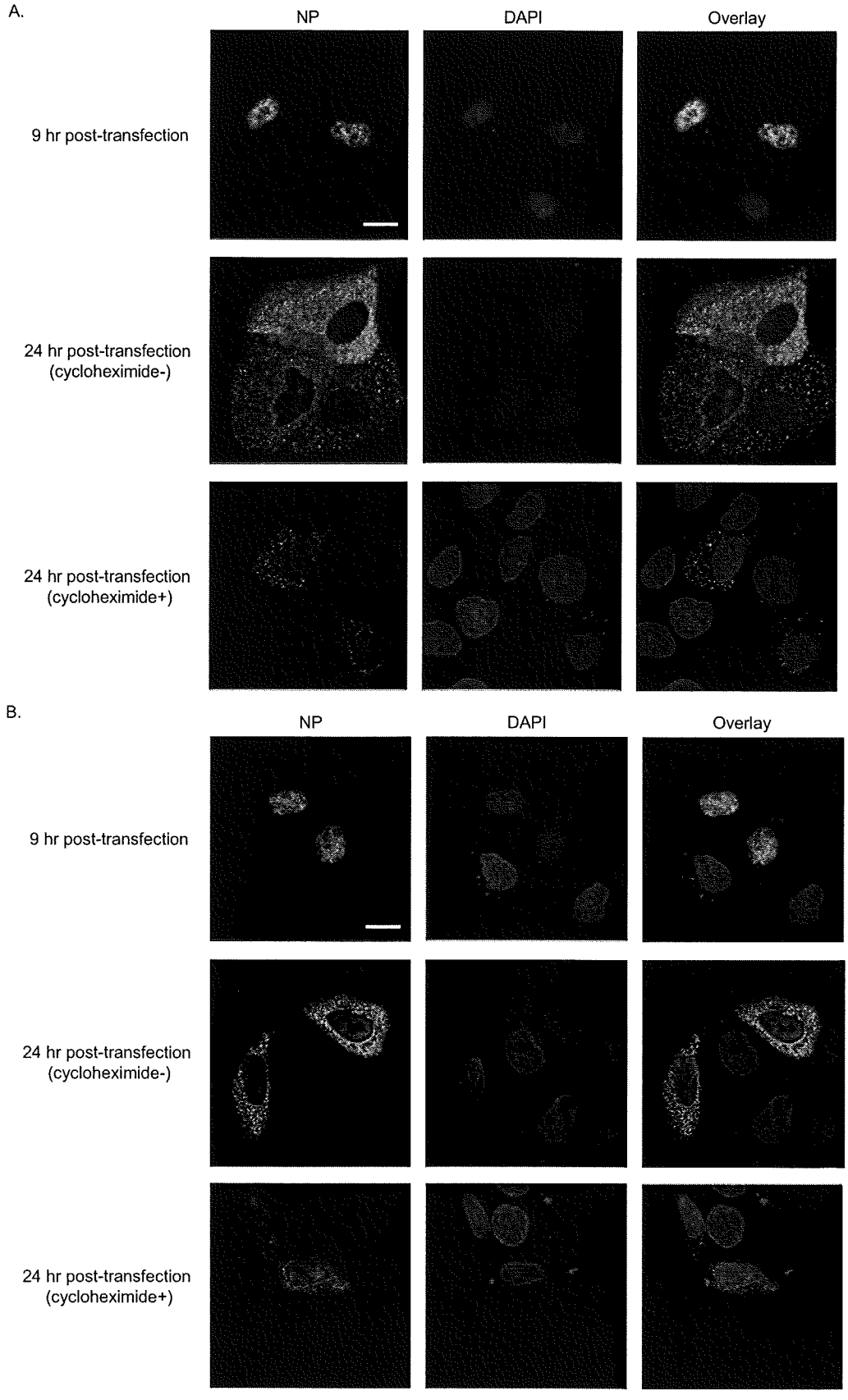

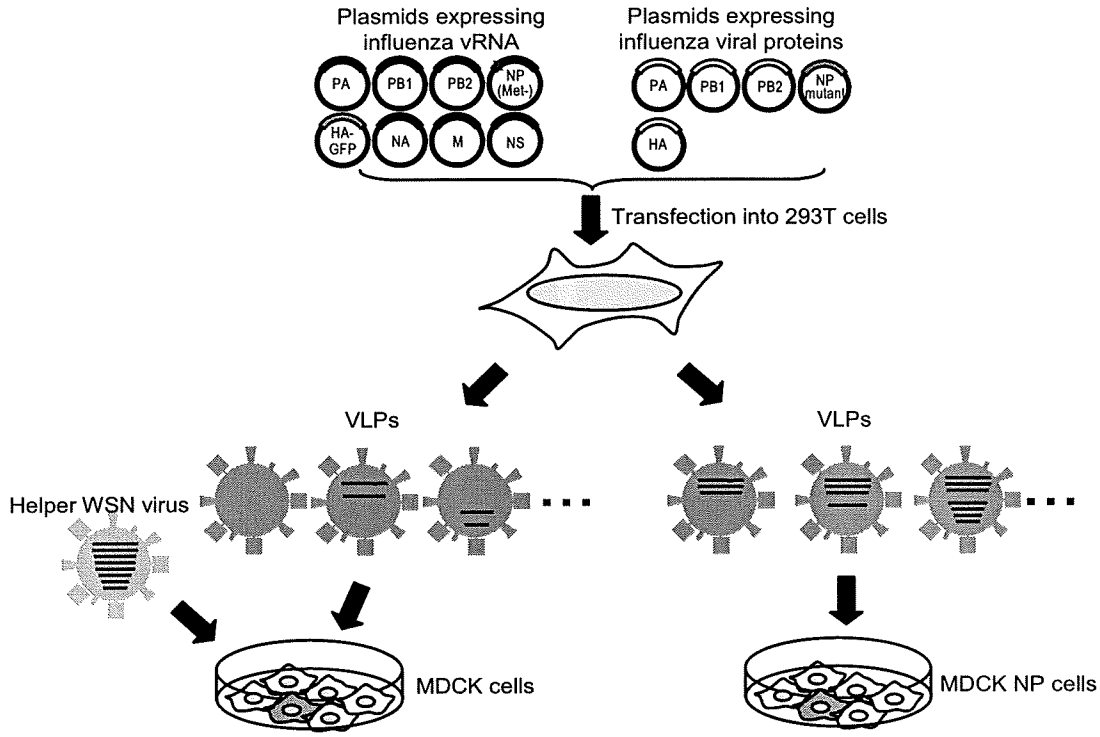

FIG. 3. System to test vRNP virion incorporation efficiencies. VLPs were recovered from 293T cells transfected with eight PolI constructs for the eight RNA segments PB1, PB2, PA, NA, M, NS, HA-GFP, and NP(Met$^-$), which lacks a start codon. These VLPs were used to infect MDCK cells in the presence of helper virus (left). In this experimental setting, GFP-positive MDCK cells are representative of VLPs that contain at least one vRNA segment (i.e., the HA-GFP vRNA). In a parallel experiment, VLPs derived from 293T cells were used to infect MDCK cells expressing NP (right). In this experimental setting, GFP-positive MDCK cells are indicative of VLPs that possess at least four vRNAs (i.e., the PB2, PB1, PA, and HA-GFP vRNAs).

parent effect on genome replication and transcription. For these variants, therefore, we assessed intracellular localization. MDCK cells were transfected with plasmids expressing mutant NPs, and indirect immunofluorescence assays were performed 9 h and 24 h after transfection. As shown in Fig. 2A and B and Fig. S1 in the supplemental material, 9 hours after transfection, wild-type NP and all NP mutants tested localized to the nuclei of transfected MDCK cells. Twenty-four hours after transfection, wild-type NP and all variants tested localized both to the nucleus and to the cytoplasm regardless of the addition of a translation inhibitor, cycloheximide. Since the localization of these mutant NPs was indistinguishable from that of the wild-type NP, their attenuated growth properties cannot be explained by defects in nuclear export.

Incorporation efficiency of a single vRNA segment into VLPs containing mutant NPs. For some NP mutants, the growth defects of the corresponding viruses cannot be explained by deficiencies in replication or intracellular transport. Therefore, we next examined the effects of the respective mutations on virus assembly. To determine the incorporation efficiency of vRNA segments into VLPs, we transfected 293T cells with eight PolI plasmids for the PB1, PB2, PA, NA, M, NS, HA-GFP, and NP(Met$^-$) vRNA segments. The NP(Met$^-$) vRNA produced an NP gene whose start codon was replaced with a stop codon to avoid expression of wild-type NP; the HA-GFP vRNA encodes the GFP reporter flanked by the packaging signals of the HA segment (36). Cells were cotransfected with five protein expression plasmids for PB1, PB2, PA, HA, and mutant or wild-type NP. The resultant VLPs were replication incompetent because they possessed mutant HA and NP vRNA segments instead of wild-type HA and NP vRNAs (Fig. 3). The supernatants of transfected cells were harvested at 48 h posttransfection and used to infect MDCK cells, together with a helper virus to provide a functional polymerase complex that supports the replication/transcription of HA-GFP vRNA. The number of VLPs containing the HA-GFP vRNA segment was

FIG. 2. Localization of NP mutants. MDCK cells transfected with plasmids expressing mutant NP or wild-type NP were subjected to indirect immunofluorescence assays. NP and DNA were stained with an anti-NP antibody and DAPI (4′,6′-diamidino-2-phenylindole), respectively. Samples were observed under a confocal laser microscope. Nine hours after transfection, wild-type and mutant NP exclusively localized to the nucleus. Shown are wild-type NP (A) and mutant R175A as a representative example of the mutants tested (B). Twenty-four hours after transfection, wild-type NP and all mutant NPs tested localized to both the nucleus and the cytoplasm, regardless of the addition of the translational inhibitor cycloheximide at 9 h posttransfection. The localization of the mutant NP proteins was indistinguishable from that of wild-type NP. Scale bars, 20 μm.

TABLE 2. Virion incorporation efficiencies of vRNA segments[a]

NP	No. of VLPs possessing at least one vRNA (per ml)[b]	No. of VLPs possessing at least four vRNAs (per ml)[c]
Wild type	31,900	17,800
D72A	450	0
R74A	62,500	390
K113A	2,160	0
R156A	167,000	11
R174A	8,980	0
R175A	100,000	0
R195A	26,200	0
R199A	51,000	0
K325A	5,700	0
R361A	21,080	0

[a] 293T cells were transfected with eight PolI constructs for eight RNA segments [i.e., PB1, PB2, PA, NA, M, NS, HA-GFP, and NP(Met$^-$), which lacks a start codon] and five protein expression constructs for PB1, PB2, PA, HA, and mutant or wild-type NP. Forty-eight hours later, VLPs were harvested, treated with TPCK trypsin, and used to determine the virion incorporation efficiencies of viral RNA segments as described in notes *b* and *c*. The results shown are representative data from three independent experiments.

[b] VLPs and WSN helper virus were used to infect MDCK cells. With helper virus providing polymerase proteins and wild-type NP, GFP-positive MDCK cells represented VLPs that possessed at least one vRNA, i.e., HA-GFP vRNA (Fig. 3).

[c] Infectious VLPs were used to infect MDCK-NP cells. In this approach, GFP expression from HA-GFP vRNA requires the expression of the PB2, PB1, and PA proteins from the respective vRNA segments. GFP-positive MDCK cells therefore represented VLPs that contained at least four vRNAs (i.e., the HA-GFP, PB1, PB2, and PA vRNAs).

determined by counting the cells expressing GFP at 16 h postinfection. As shown in Table 2, the number of VLPs possessing HA-GFP vRNA produced from cells expressing R74A, R156A, R175A, R195A, R199A, or R361A was at least as high as that from cells expressing wild-type NP. These results suggest that the mutations had no or little effect on the incorporation efficiency of a single vRNA segment into VLPs. In contrast, cells expressing D72A, K113A, R174A, or K325A produced VLPs containing HA-GFP vRNA less efficiently than did the wild-type NP, indicating that these NP mutations may impair vRNA incorporation into VLPs, resulting in the observed failure of virus rescue.

Incorporation efficiency of multiple vRNA segments into VLPs containing mutant NPs. As described above, we found that R74A, R156A, R175A, R195A, R199A, and R361A support VLP incorporation of a single vRNA segment, leaving in question why these viruses replicate poorly. A possible explanation is that the NP mutant facilitates virion incorporation of single, but not multiple, vRNA segment. In such a scenario, the NP would assemble vRNA segments into sets of eight (in the form of RNPs) that constitute a functional genome. To examine this possibility, we generated an MDCK cell line stably expressing wild-type NP and used the cell line for VLP infection. Since a helper virus was not used for this experiment, PA, PB1, and PB2 vRNA segments had to be provided by incoming VLPs to support the replication/transcription of HA-GFP vRNA. The number of GFP-expressing cells should, therefore, correspond to the number of VLPs possessing at least four vRNAs (i.e., PA, PB1, PB2, and HA-GFP vRNAs). As shown in Table 2, we found that the number of VLPs possessing at least four vRNAs produced from cells expressing R74A, R156A, R175A, R195A, R199A, or R361A was significantly lower than that from cells expressing wild-type NP. These results suggest that these mutations affect the efficient incorporation of multiple vRNA segments into VLPs, even though they had no or little effect on the virion incorporation of a single vRNA. As expected, the mutations D72A, K113A, R174A, and K325A completely inhibited VLP incorporation of four vRNAs.

DISCUSSION

In this study, we conducted a comprehensive mutational analysis to examine the roles of highly conserved amino acids in the influenza A virus NP for the virus life cycle. We found 17 amino acid substitutions (i.e., R19A, Y40A, L49A, R98A, G132A, S141A, G169A, R214A, V242A, P277A, F291A, N319A, C333A, K357A, E369A, G490A, and E495E) that had no or little effect on virus growth in vitro at either 33°C or 37°C, whereas other mutations tested significantly impaired viral replication efficiency. Using an in vitro replication assay, we identified 15 amino acid changes (i.e., R150A, R208A, R213A, E254A, A260R, K273A, A337R, E339A, R355A, A387R, Q405A, F412A, R416A, F488A, and F489A) that are crucial for viral-genome replication and/or transcription (Table 1). Several NP mutants supported efficient replication in an in vitro replication assay but were highly attenuated in their growth properties. Some of these mutants facilitated efficient virion incorporation of a single vRNA but not that of multiple vRNAs. This is the first report that suggests a role of an influenza virus protein in the assembly and/or virion incorporation of vRNA segments.

The genome of influenza A virus consists of eight RNA segments. Two packaging models have been proposed for the generation of infectious virions containing these eight vRNA segments: "random-packaging" and "selective-packaging" models (9, 10, 37). Recently, it has been suggested that each vRNA segment of influenza A viruses contains specific incorporation signals for the recruitment and/or packaging of vRNPs into virions (6, 7, 11–13, 20, 21, 28, 36). These data support the "selective-packaging" mechanism of vRNA recruitment into virions. However, the involvement of other factors (i.e., viral proteins and/or host proteins) in the selective incorporation of the eight vRNPs into progeny virions is still poorly understood. In this study, we found 10 mutations (D72A, R74A, K113A, R156A, R174A, R175A, R195A, R199A, K325A, and R361A) that impaired the efficient incorporation of a set of at least four vRNAs (PA, PB1, PB2, and HA-GFP vRNP) into VLPs, although they did not affect the VLP incorporation of a single vRNA, i.e., the HA-GFP vRNA (Table 2). As shown in Fig. 4, eight of these NP mutations (i.e., D72A, K113A, R156A, R174A, R175A, R195A, R199A, and R361A) cluster around a possible RNA-binding groove that lies between the head and body domains at the exterior of the NP oligomer and is lined with highly conserved basic residues (41). Two of these residues (R74 and K325) are located in an internal domain of NP. The architecture of RNP complexes in influenza A virus particles is such that the RNPs are organized in a distinct pattern of seven segments of different lengths surrounding a central segment. Close contact has been shown between the peripheral RNPs, as well as the central and peripheral RNPs (26). NP may be involved in this close contact among the peripheral RNPs,